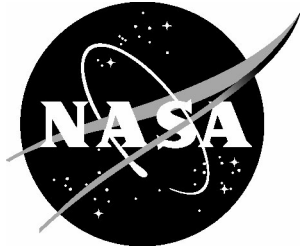


NASA/CR-2003-212679



# Automated Finite Element Analysis of Elastically-Tailored Plates

*Brian F. Tatting*  
*ADOPTTECH, Inc., Blacksburg, Virginia*

*Zafer Gürdal*  
*Virginia Polytechnic Institute and State University, Blacksburg, Virginia*

## The NASA STI Program Office . . . in Profile

Since its founding, NASA has been dedicated to the advancement of aeronautics and space science. The NASA Scientific and Technical Information (STI) Program Office plays a key part in helping NASA maintain this important role.

The NASA STI Program Office is operated by Langley Research Center, the lead center for NASA's scientific and technical information. The NASA STI Program Office provides access to the NASA STI Database, the largest collection of aeronautical and space science STI in the world. The Program Office is also NASA's institutional mechanism for disseminating the results of its research and development activities. These results are published by NASA in the NASA STI Report Series, which includes the following report types:

- **TECHNICAL PUBLICATION.** Reports of completed research or a major significant phase of research that present the results of NASA programs and include extensive data or theoretical analysis. Includes compilations of significant scientific and technical data and information deemed to be of continuing reference value. NASA counterpart of peer-reviewed formal professional papers, but having less stringent limitations on manuscript length and extent of graphic presentations.
- **TECHNICAL MEMORANDUM.** Scientific and technical findings that are preliminary or of specialized interest, e.g., quick release reports, working papers, and bibliographies that contain minimal annotation. Does not contain extensive analysis.
- **CONTRACTOR REPORT.** Scientific and technical findings by NASA-sponsored contractors and grantees.

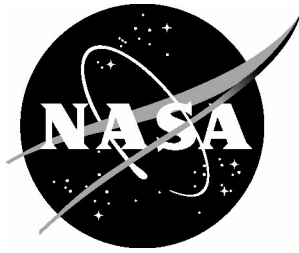
- **CONFERENCE PUBLICATION.** Collected papers from scientific and technical conferences, symposia, seminars, or other meetings sponsored or co-sponsored by NASA.
- **SPECIAL PUBLICATION.** Scientific, technical, or historical information from NASA programs, projects, and missions, often concerned with subjects having substantial public interest.
- **TECHNICAL TRANSLATION.** English-language translations of foreign scientific and technical material pertinent to NASA's mission.

Specialized services that complement the STI Program Office's diverse offerings include creating custom thesauri, building customized databases, organizing and publishing research results ... even providing videos.

For more information about the NASA STI Program Office, see the following:

- Access the NASA STI Program Home Page at [\*http://www.sti.nasa.gov\*](http://www.sti.nasa.gov)
- E-mail your question via the Internet to [\*help@sti.nasa.gov\*](mailto:help@sti.nasa.gov)
- Fax your question to the NASA STI Help Desk at (301) 621-0134
- Phone the NASA STI Help Desk at (301) 621-0390
- Write to:  
NASA STI Help Desk  
NASA Center for AeroSpace Information  
7121 Standard Drive  
Hanover, MD 21076-1320

NASA/CR-2003-212679



# Automated Finite Element Analysis of Elastically-Tailored Plates

*Brian F. Tatting*  
*ADOPTTECH, Inc., Blacksburg, Virginia*

*Zafer Gürdal*  
*Virginia Polytechnic Institute and State University, Blacksburg, Virginia*

National Aeronautics and  
Space Administration

Langley Research Center  
Hampton, Virginia 23681-2199

Prepared for Langley Research Center  
under Contract NAS1-00135

December 2003

## Acknowledgments

The authors would like to acknowledge the assistance of those individuals who aided in the preparation of this document. The original guidance of James H. Starnes, Jr., of NASA-Langley Research Center, provided the initial encouragement for this investigation into the variable stiffness concepts. Additional support by personnel at NASA-Langley, namely Damodar Ambur and Dawn Jegley, was instrumental in furthering the curvilinear fiber research of the authors. Dawn Jegley of NASA-Langley was the grant monitor for this task and also helped review this document. Grant Soremekun and Scott Ragon of ADOPTTECH provided project support and guidance and supplied useful explanations into the working of the *OLGA* software.

|   |
|---|
| The use of trademarks or names of manufacturers in the report is for accurate reporting and does not constitute an official endorsement, either expressed or implied, of such products or manufacturers by the National Aeronautics and Space Administration. |
|---|

Available from:

NASA Center for AeroSpace Information (CASI)  
7121 Standard Drive  
Hanover, MD 21076-1320  
(301) 621-0390

National Technical Information Service (NTIS)  
5285 Port Royal Road  
Springfield, VA 22161-2171  
(703) 605-6000

## Abstract

A procedure for analyzing and designing elastically tailored composite laminates using the *STAGS* finite element solver has been presented. The methodology used to produce the elastic tailoring, namely computer-controlled steering of unidirectionally reinforced composite material tows, has been reduced to a handful of design parameters along with a selection of construction methods. The generality of the tow-steered ply definition provides the user a wide variety of options for laminate design, which can be automatically incorporated with any finite element model that is composed of *STAGS* shell elements. Furthermore, the variable stiffness parameterization is formulated so that manufacturability can be assessed during the design process, plus new ideas using tow-steering concepts can be easily integrated within the general framework of the elastic tailoring definitions. Details for the necessary implementation of the tow-steering definitions within the *STAGS* hierarchy are provided, and the format of the ply definitions is discussed in detail to provide easy access to the elastic tailoring choices. Integration of the automated *STAGS* solver with laminate design software has been demonstrated, so that the large design space generated by the tow-steering options can be traversed effectively. Several design problems are presented which confirm the usefulness of the design tool as well as further establish the potential of tow-steered plies for laminate design.

## 1.0 Introduction

Elastic tailoring implies that the stiffness response of a structure can be modified to improve its performance, measured through increased load-carrying capability or lower weight for a specified design load. Generally, elastic tailoring is accomplished through alteration of the characteristics of the material used for construction. Though numerous possibilities exist under this field of study, attention is focused here on the design of fiber-reinforced composite materials through the use of curvilinear fiber paths. Traditionally, design of fiber-reinforced laminates is limited to through-the-thickness optimization of stacking sequences for thin laminates, where each layer is constructed of straight fiber directional materials. However, it has long been realized that in-plane variation of the fiber directions produces a greater efficiency for the placement of the stiff and strong fibers that constitute the composite material.<sup>1-5</sup> Therefore, this document builds on earlier work by the present authors<sup>6</sup> that uses generalized curvilinear fiber path definitions to provide a practical means for the analysis and design of elastically tailored laminates. For this phase of the research, development of an automated finite element analysis of laminates using the curvilinear fiber definitions is the main focus. Integration of the tool with an existing design environment is also accomplished, and several design examples are provided to illustrate the effectiveness of the design technique and demonstrate the potential of the elastic tailoring method.

## 2.0 Elastic Tailoring through Tow Steering

The mechanism used here to tailor stiffness within a structure is based on laminates constructed of plies that utilize curvilinear fiber paths. The first section of this chapter introduces the fabrication method behind this technique, namely the automated placement of fibers using advanced tow placement delivery systems. The parameterization of a tow-steered ply is then outlined, where the definition of the curvilinear paths adheres to the capabilities and constraints of a standard tow placement machine. The formulation uses a linear variation of the fiber orientation angle as the basis of the elastically-tailored ply, though the scheme is organized so that alternate definitions can be easily incorporated. Several ply construction methods using the tow-steered ply parameterization are presented, and some specific characteristics inherent to tow-steered laminates are discussed.

### 2.1 Tow Steering Capabilities and Manufacturing Constraints

The tow placement machine that will serve as the basis for discussion is the *VIPER FPS-3000* Fiber Placement System, manufactured by Cincinnati Machine.<sup>7</sup> This system has been used by the present

authors in the past to manufacture flat laminates using curvilinear fibers.<sup>8</sup> A photograph of the tow placement machine head is shown in Figure 1. A schematic of the operating principle behind the placement of the tows is displayed in Figure 2. The material is supplied in spools of slit tape, 0.125 inches wide for this machine. Up to 32 individual tows<sup>†</sup> can be controlled by the fiber placement head at one time, which can be dispensed at different speeds to enable curved paths to be applied to a surface. Cutting and restarting of each tow can also be performed independently. During application, the tows are advanced through a feeding mechanism and applied to the surface while being heated and compacted by the machine applicator head. Each path traversed by the tow placement head which lays down any number of tows is termed a *course*, and a set of courses arranged to cover a defined area makes up a ply. The seven-axis machine allows for complex convex and concave surfaces to be covered by multiple plies to make up a laminate, and the entire process is controlled by *ACRAPLACE* software, which is able to model the tow placement process before production to ensure feasibility of the coverage technique. Due to the precision of the computer-controlled environment, accurate estimates of the fiber orientation angles within the laminate are available for all points on the surface. Similarly, the system is flexible enough to allow user-defined tow paths to be directly transformed into data that can be accessed by the *ACRAPLACE* software, so that excellent agreement can be maintained between theoretical designs and prototype parts.

Previous production of parts using curvilinear fibers has revealed several important constraints that must be accounted for during the design process. The major limiting factor concerns the turning radius of the tow placement head. Too small of a turning radius causes the inner tows to wrinkle, which is detrimental to the quality of the finished part. For a flat mandrel, the limiting turning radius for the tow placement machine when controlling 24 tows is estimated by the manufacturer to be 25 inches. The other noteworthy manufacturing constraint for curvilinear fiber paths is the minimum cut length parameter. Minimum cut length refers to the distance between the material feed and the tow cutting mechanism within the tow placement head. Each tow that is started and later cut must surpass this minimum length requirement so that the tow placement head can correctly position the ply. Too short of a tow segment will not reach the compaction head, which holds the tow against the surface while the other end is being cut. Plies that utilize tow dropping must be examined so that this minimum cut length is achieved, else areas lacking fibers will occur within the laminate. The minimum cut length for the tow placement machine used here is 5 inches. Both the minimum cut length and curvature constraint are evaluated by the *ACRAPLACE* software before production to ensure that the coverage pattern is acceptable. Thus it is advantageous to understand these manufacturing constraints beforehand so that they can be taken into account during the design phase.

An interesting feature that was considered during manufacturing for earlier work<sup>8</sup> involves the possibility of terminating a tow when a limiting curve is approached at an odd angle. This limiting curve could be a neighboring course that is not exactly perpendicular to the one being laid down, or the bounding edge of the laminate. As the course approaches this limiting curve, tows are successively cut as they approach the curve boundary, which ensures the necessary coverage of the area yet saves on the amount of material that is being used. In tow-placement fabrication terminology, this is referred to as the *coverage*. For 0% coverage, each tow is cut so that their leading edge does not extend past the limiting curve, as shown in Figure 3a. Small wedge-like gaps, represented by the gray areas in the figure, occur due to the discrete perpendicular cut of each tow. 50% coverage directs the tow drop to occur so that the center of the tow ends at the limiting curve, as shown in Figure 3b. Lastly, 100% coverage delays the dropping of the tow until the limiting curve is passed, ensuring that the entire gap is covered with fiber material. However, the two latter coverage methods can lead to a slight build-up in thickness if the limiting curve is another course. As we will demonstrate in Section 2.2.3, the presence of curvilinear plies can lead to the necessity of tow drops between neighboring courses, which provides the opportunity to alter the coverage

---

<sup>†</sup> For this study, 24 tows were assumed to be used for manufacture, due to the availability of machine constraint information for this configuration and the fact that earlier laminates were constructed using the number of tows.

parameter in this manner. It was at first decided that the 0% coverage option was preferred for such a situation since entirely flat laminates were most desirable. However, the amount of overlap possible with the curvilinear fiber format suggested that this gradual thickness build-up may lead to a desirable feature in the form of an integrally stiffened region within the laminate. Consequently, tow-steered laminates were fabricated allowing these full overlaps between neighboring curvilinear courses. A photograph of a finished part that allowed these full overlaps is shown in Figure 4. Testing revealed that these integrally stiffened sections did provide a significant increase in structural performance,<sup>9,10</sup> therefore subsequent research in this area continued to use these thickness build-ups. A staggering technique was also devised in the earlier stages of this project<sup>6</sup> to smooth out some of the more drastic thickness disparities and produce a laminate with variable thickness. A photograph of such a laminate, along with a numerical representation of the thickness variation, is shown in Figure 5. The figure on the right is a contour plot of the number of plies present within the laminate, which ranges from 20 to 28 plies yet does so smoothly so that the variation is hard to discern in practice. Design of laminates incorporating this novel laminate feature is one of the accomplishments of this research, and explained in detail in the following chapters.

## 2.2 Parameterization of Tow Steered Ply

The capabilities of modern tow-placement machines provide the designer a multitude of choices for the directions and variations of the tow paths. For example, design variables could be based on fiber orientation angles at various independent locations within the structure, resulting in a laminate that is, in essence, designed locally according to the stress state at that location. However, this luxury is often disadvantageous in a design environment since it leads to a large and varied design space that makes it difficult for the optimization algorithm to converge to a useful solution, as well as the difficulty of transforming the design into an actual part that can be manufactured using the tow-steering process. Therefore, some restrictions on the available tow paths are required to better pose the resulting optimization problem in terms of a smaller set of design variables. These design parameters should also reflect the manufacturability of a tow-placed ply, discussed in section 2.1, by being based on quantities that can be directly translated into data that can be understood by the tow-placement machine. Furthermore, during analysis it will be required to calculate the actual stacking sequence at any location within the structure, therefore the parameterization is presented with a formalized solution for an arbitrary material point in mind. The following sections provide the details for the parameterization used in this research.

### 2.2.1 Fabrication Coordinates

The fabrication technique of modern tow-placement machines is based on laying down a series of layers over the surface of a mandrel. Therefore, for thin laminates the computer-controlled machine can be envisioned to be working over the geometric surface of the structure, and tow paths defined in terms of these surface coordinates can be easily transformed into readable data for the manufacturing phase. Designation of these surface coordinates is usually based on the principal directions associated with the surface geometry, which reduces three-dimensional structures into ones defined by two surface coordinates, designated here as  $\xi$  and  $\psi$ , with the third direction ( $z$ ) assumed to be normal to the surface at all locations. For general structures, such as flat plates and cylindrical panels and shells, the transformation from surface coordinates to the three-dimensional definition is quite straightforward, and for more complex surfaces numerical algorithms must be available to perform this transformation. *Fabrication coordinates*, designated herein as  $x$  and  $y$ , are based on these surface coordinates with the extra stipulation that the fabrication coordinates possess units in terms of length. For example, surface coordinates for a circular cylindrical shell are often defined in terms of the axial location ( $\xi$ ) and circumferential angle ( $\psi$ ). Transformation to fabrication coordinates would not be required for the axial coordinate since it is already defined in terms of length ( $x = \xi$ ), while in the circumferential direction the angle would need to be transformed to an arc-length quantity in the usual manner ( $y = R\psi$ , where  $R$  is the

radius of the cylinder). The tow path definitions defined in this report will always be based on these fabrication coordinates for ease of expression, and it will be assumed that the appropriate transformations can be performed for the structure under consideration.

### 2.2.2 Reference Path Designation

To aid in the definition of a tow-steered ply and the subsequent solution for the local fiber orientation angles, a reference path based on a minimum number of parameters is defined in terms of the fabrication coordinates. However, some generality is introduced to accommodate future reference path definitions that may be needed for specific geometries. This is accomplished by separating the definition into three stages. In the first stage, a reference path is defined as a single-valued function within a two-dimensional domain. Relations for the orientation angle and curvature of this path are also calculated. In a physical sense, this reference path represents the curve traversed by the center of the applicator head of the tow-placement machine during the fabrication of a single course. In the second stage, equations that determine necessary parameters for an arbitrary point that is perpendicular to some point on the reference path are formulated. This stage represents the calculations required to determine the orientation angle for a material point within the course, which has a given width due to the multiple tows within the applicator head. The final stage employs a global translation and rotation to transform all of the points within each course to the fabrication axes, which are directly related to the surface coordinates within the structure as discussed in the previous section. The relevant equations for these stages are presented in reverse order, so that the transformation from fabrication coordinates to the reference path definition is made clear.

Since the fabrication coordinates are based on the surface geometry of the structure, transformations are applied for translation and rotation which enable the path definition to be moved and rotated easily within the domain of the structure. This feature is quite useful for aligning the tow-steered plies to the structure's coordinate system and for performing simple translational and rotational changes to the curvilinear plies (such as those needed for the staggering technique mentioned in Section 2.1), and represents the third stage of the tow-steered ply definition. The new coordinates  $\{x', y'\}$  that arise due to this transformation are termed *directional coordinates*, and represent the origin and major direction of the stiffness variation. Variables in the directional coordinate domain are denoted by a prime ( $'$ ). The transformations between the fabrication and directional coordinates are demonstrated graphically in Figure 6 and given below for a translation of  $\{x_0, y_0\}$  and a rotation  $\phi$ , along with equations that relate the local fiber orientation directions ( $\theta$ ) and curvatures ( $\kappa$ ) in each coordinate system (these extra parameters being significant for calculations introduced later):

$$\begin{aligned} x &= x_0 + x' \cos \phi - y' \sin \phi & x' &= (x - x_0) \cos \phi + (y - y_0) \sin \phi \\ y &= y_0 + x' \sin \phi + y' \cos \phi & y' &= -(x - x_0) \sin \phi + (y - y_0) \cos \phi \\ \theta(x, y) &= \phi + \theta'(x', y') & \theta'(x', y') &= \phi - \theta(x, y) \\ \kappa(x, y) &= \kappa'(x', y') & \kappa'(x', y') &= \kappa(x, y) \end{aligned} \quad (2.1)$$

Within the directional coordinate space, there exists a reference curve that will serve as the basis for the tow-steered ply definition. As mentioned earlier, the curve is defined as a single-valued function in terms of a one-dimensional coordinate  $x^*$ , where the asterisk ( $*$ ) denotes that the variable is associated with the reference curve function. For this stage of the calculations, the reference curve function is considered arbitrary and it is assumed that calculations for the single-valued function  $y^*(x^*)$ , tangent angle to the curve  $\theta^*(x^*)$ , and curvature  $\kappa^*(x^*)$  exist for all  $x^*$ . Under these conditions, a point  $P$  in  $\{x', y'\}$  space can be defined in terms of a point on the reference curve, denoted by  $\{x^*, y^*(x^*)\}$ , and the perpendicular distance ( $r$ ) to that point. These quantities are displayed in Figure 7, and the corresponding equations are



$$\begin{aligned}
x' &= x^* - r \sin \tilde{\theta}(x^*) & \theta'(x', y') &= \theta^*(x^*) \\
y' &= y^*(x^*) + r \cos \tilde{\theta}(x^*) & \kappa'(x', y') &= \kappa^*(x^*) / [1 - r \kappa^*(x^*)]
\end{aligned} \tag{2.2}$$

Inversion of the first two equations in (2.2) results in two equations for the variables  $x^*$  and  $r$ :

$$\begin{aligned}
r &= (y' - y^*) \cos \theta^* - (x' - x^*) \sin \theta^* \\
(x' - x^*) \cos \theta^* + (y' - y^*) \sin \theta^* &= 0
\end{aligned} \tag{2.3}$$

Note that for a given point in prime coordinates, the latter equation can be solved once the function for the reference curve is defined, and the solution for  $r$  in the former equation is then easily determined from the reference curve functions. It should also be noted here that, in general, equations (2.3) are nonlinear and therefore more than one solution may exist. This usually means that either the reference curve functions are not well chosen, or more likely that the point in prime space is a center of curvature. This latter condition indicates that the reference curve definition is invalid, since it leads to multiple locations on the reference curve that are equidistant from the point under consideration. Further discussion of this condition with respect to the manufacturing curvature constraint will be postponed until section 2.2.3.

The last equations to be formulated are those for the reference curve. The objective of the definition is to determine a manageable set of parameters that can represent an arbitrary curve in two-dimensional space. One such variation, originally introduced by Gürdal,<sup>11,12</sup> is based on a linear saw-tooth variation of the tangent angle of the curve (here often referred to as the orientation angle), which requires three parameters for a complete definition. A graphical representation of the reference curve function and orientation angle variation is shown in Figure 8. The first parameter,  $T_0$ , represents the orientation angle at the origin of the directional coordinate axis. At a certain distance  $d$  along the abscissa, a second orientation angle  $T_1$  is defined. The variation of the orientation angle between these two points is assumed linear, and the function is repeating and symmetric about the origin to cover the entire domain. This variation can be represented mathematically as

$$\theta^*(x^*) = \begin{cases} T_0 + (T_1 - T_0) \left( \frac{x^*}{d} - k \right), & k \text{ even} \\ T_1 + (T_0 - T_1) \left( \frac{x^*}{d} - k \right), & k \text{ odd} \end{cases}, \quad k = \text{floor} \left[ \frac{x^*}{d} \right], \tag{2.4}$$

where the *floor* function truncates the real number to the nearest integer that is less than or equal to it. The equation for a point on the curve is found through integration,

$$y^*(x^*) = \begin{cases} kS + \frac{d}{(T_0 - T_1)} \ln \left[ \frac{\cos \theta^*}{\cos T_0} \right], & k \text{ even} \\ kS + \frac{d}{(T_1 - T_0)} \ln \left[ \frac{\cos \theta^*}{\cos T_1} \right], & k \text{ odd} \end{cases}, \quad k = \text{floor} \left[ \frac{x^*}{d} \right], \quad S = \frac{d}{(T_0 - T_1)} \ln \left[ \frac{\cos T_1}{\cos T_0} \right]. \tag{2.5}$$

Two special cases exist for this reference curve definition. First, if the orientation angles  $T_0$  and  $T_1$  are equal, the resulting curve is a straight line defined by

$$y^*(x^*) = x^* \tan T_0, \quad \text{if } T_0 = T_1. \tag{2.6}$$

Secondly, if the orientation angles differ they both must be constrained to be between  $-\pi/2$  and  $\pi/2$  (or  $-90^\circ$  and  $90^\circ$ ), else the calculation for the parametric curve in (2.5) is incalculable. Note also that to solve

the second equation in (2.3) for a given point in the prime space, a nonlinear iterative procedure must be used to find  $x^*$ . This is due to the complexity of equation (2.5).<sup>‡</sup>

The local curvature of the reference path curve is found from equation (2.4) through differentiation. The local curvature is inversely related to the turning radius along the curve, and is used to estimate the feasibility of the tow-steered ply definition with respect to the minimum allowable turning radius of the tow-placement machine. The relation for the curvature is given as

$$\kappa^*(x^*) = \frac{\frac{d}{dx^*}(\tan \theta^*)}{(1 + \tan^2 \theta^*)^{3/2}} = \frac{(-1)^k (T_1 - T_0)}{d} \cos \theta^*(x^*), \quad k = \text{floor} \left[ \frac{x^*}{d} \right]. \quad (2.7)$$

Note that the equation varies with respect to  $x^*$ , so that in general the entire curve from 0 to  $d$  must be investigated to determine the maximum curvature for the path. However, in practice it is easily seen that the maximum value must occur where  $\cos \theta^*(x^*)$  is a maximum, which is either 0,  $T_0$  or  $T_1$  due to the definition of the orientation angle variation given in (2.4).

Equations (2.1) through (2.7) provide methods to calculate the orientation angle for a point given in fabrication coordinates based on a reference path defined by six parameters ( $\{x_0, y_0\}$ ,  $\phi$ ,  $T_0$ ,  $d$ , and  $T_1$ ). The organization of the parameters allows modifications to the definitions (such as a different basis for the angle variation) without having to re-formulate the basic algorithms already in place. Furthermore, the set of design parameters represented by  $\phi$ ,  $T_0$ , and  $T_1$  provides a wide variety of reference path variations without dramatically increasing the design space. Section 2.2.3 details techniques to transform these reference path definitions into plies that cover the entire domain of the structure.

### 2.2.3 Ply Construction Methods

The reference path definition presented in the previous section provides the necessary equations to calculate one path of the centerline of the applicator head of the tow placement machine. The applicator head has a finite width dependent on the number of tows used, and one pass of the head across the surface of the part lays down a single band of material (referred to as a *course*). To completely cover the entire structure, additional courses must be laid. These courses are defined with respect to the reference curve already defined, however there are several different methods available to fulfill this objective.

The first, most obvious ply construction technique is referred to as the *parallel* method, and consists of laying down additional courses that line up exactly with the edges of previous courses. This implies that no gaps occur between courses, which leads to a constant thickness ply that possesses a stiffness definition with roughly the same degree of variation in both fabrication directions. Mathematically, a new parallel course is defined from the reference path through the perpendicular distance variable  $r$  in equations (2.2) and (2.3). For each course, the limits on  $r$  range from  $(j-1/2)$  to  $(j+1/2)$  multiplied by the total

---

<sup>‡</sup> It should be noted here that the reason for choosing the linear variation of the orientation angle as the basis for the reference path variation is due to its use in earlier research by these authors. Originally, closed-form solutions were sought for rectangular plates with simple boundary conditions, and the linear variation of the orientation angle was required so that integration of laminate stiffness terms could be performed analytically. Recently, a more applicable reference path function has been developed, which yields a simpler solution for equation (2.5) and removes the need for an iterative nonlinear solver. The new definition is based on circular arcs instead of a linear variation of the orientation angle, and can be formulated using the same three parameters  $T_0$ ,  $T_1$ , and  $d$ . Besides generating more efficient solution algorithms, this definition also has the advantage of producing courses of constant curvature, which better corresponds to the manufacturing constraints of a tow-placement machine. In the future, the constant curvature path will be used in favor of the linear variation of the orientation angle, yet to do so in this document would invalidate comparisons to earlier analytically and experimental results.

width of the applicator head  $h$ , where  $j$  is identified as the course ID and is zero for the reference path. Several example courses for the parallel method are displayed in Figure 9, where the dashed lines are the centerlines and the solid lines are the outer limits of each course. To determine the fiber orientation angle for an arbitrary point within a parallel method ply, the equations of the previous section can be used. The perpendicular distance variable  $r$  determines within which course the point lies, and also aids in determining the local curvature at that point through the last equation of (2.2). For a center of curvature, the denominator for the curvature equation in (2.2) is identically zero, which leads to an infeasible design. Moreover, a curvature value that exceeds the constraint value for the tow placement machine also implies that the ply cannot be manufactured using the present techniques. In practice, infeasibility is more easily estimated by determining the center of curvature for each point along the reference curve. Each center of curvature has a corresponding minimum turning radius within the structure that lies on a centerline of a course, and the smallest turning radius within this set is used to determine the manufacturing feasibility.

The main disadvantage of the parallel ply construction method is that tow-steered plies that possess a large stiffness variation tend to be infeasible due to the smaller turning radius required for subsequent courses. In contrast, *shifted* methods utilize copies of the reference path for the additional courses, which allows for greater stiffness variation and more feasible designs (especially for larger structures). An example of a shifted course is shown in Figure 10, where a new course, identical in shape to the reference path, is laid down next to the reference course but shifted a distance  $s$  perpendicular to the variation direction (along the  $y'$  coordinate). Due to the curvature of the path, the top of one course does not match up with the bottom of a neighboring course for all  $x'$  locations, which leads to an irregular region between neighboring courses. This region can be accounted for in various ways. On one extreme, the shift distance  $s$  is prescribed so that no overlap exists and a gap containing no material is present between adjacent courses. Such a configuration is displayed in Figure 10. The contrasting case has a shift distance defined to remove the gaps between the courses and to minimize the overlap. This is accomplished by choosing  $s$  so that the courses abut at the  $x'$  location that produces the largest gap, as shown in Figure 11. This produces an overlap region for curved reference paths (though both configurations yield no overlaps or gaps for straight reference paths,  $T_0 = T_1$ ). In practice, the latter case is most often used so that no gaps occur within a ply. For such a case, the shift distance  $s$  is calculated automatically once the reference curve parameters are defined, though an option exists to increase/decrease the shift amount for specialized configurations. As compared to the parallel method, shifted methods tend to produce a predominantly unidirectional stiffness variation along the  $\phi$ -direction.

Within the overlap regions of a ply using the shifted technique, the tow placement machine can be instructed to drop tows individually so that no thickness build-up occurs (referred to as the *tow-drop* method); or allow overlaps from successive courses to produce areas of increased thickness. This latter configuration has been dubbed the *overlap* method, and is a novel way to introduce thicker regions within a laminate that act like local stiffeners. Close-ups of the overlap region for both methods, using typical values for the reference curve parameters, are shown in Figure 12. Each tow within a course is shown individually to illustrate the condition within the overlap region. Note that slight gaps still exist for the tow-drop method due to the discrete nature of dropping and adding tows. Decisions on when to drop tows from each course are made based on minimizing these gaps as well as the minimum cut length manufacturing constraint and the coverage parameter (discussed in Section 2.1). Manufacturing constraints in terms of curvature need to be satisfied for the reference curve only (calculated from the maximum value of equation (2.7)), which leads to a greater availability of feasible design choices. Calculations for the orientation angle at a certain  $\{x, y\}$  point are again based on the equations of the previous section, though now a new additive term must be included within the  $y'$  equation in (2.2) to account for the shifted course. For the tow-drop method, the orientation angle is based on the course that is nearest to the point under consideration, while for the overlap method multiple orientation angles (configured as additional layers within the laminate) can be defined for points that lay within the overlap regions.

## 2.3 Tow Steered Laminates

Laminates composed of tow-steered plies possess some characteristics that do not exist for traditional constant stiffness plies. These differences are most apparent when traditional laminate stiffness properties are calculated. Here these properties are referred to as the extensional stiffness matrix  $[A]$ , coupling stiffness matrix  $[B]$ , and bending stiffness matrix  $[D]$ . Each matrix has order  $3 \times 3$  and is symmetric, containing six terms that are dependent on the unidirectional elastic material properties and stacking sequence of the laminate. Subscripts for each term denote its association with specific types of deformation, with <sub>1</sub> traditionally corresponding to the  $x$ -direction extension, <sub>2</sub> for  $y$ -direction extension, and <sub>6</sub> for in-plane shear deformation. Standard representation of the (symmetric) matrices is given as

$$[A] = \begin{bmatrix} A_{11} & A_{12} & A_{16} \\ A_{12} & A_{22} & A_{26} \\ A_{16} & A_{26} & A_{66} \end{bmatrix}, \quad [B] = \begin{bmatrix} B_{11} & B_{12} & B_{16} \\ B_{12} & B_{22} & B_{26} \\ B_{16} & B_{26} & B_{66} \end{bmatrix}, \quad [D] = \begin{bmatrix} D_{11} & D_{12} & D_{16} \\ D_{12} & D_{22} & D_{26} \\ D_{16} & D_{26} & D_{66} \end{bmatrix}. \quad (2.8)$$

Laminates are generally composed of multiple isotropic or orthotropic layers, with each having independent material properties, ply thickness, and orientation angle. For the laminates considered here, the material choice and ply thickness are the same for each layer, so that the stacking sequence is used to differentiate designs by designating the order of the orientation angles through the thickness of the laminate. Stacking sequences are grouped within brackets, with the list of orientation angles recorded in degrees with respect to the  $x$ -axis, starting at the bottom of the laminate and separated by slashes. Adjacent plies with identical orientation angle definitions can be grouped with numerical subscripts, while layers of opposite sign can be denoted with the symbol  $\pm$ . For example, a stacking sequence expressed as  $[\pm 45_2/90_2/0]$  consists of seven plies with  $\{+45^\circ, -45^\circ, +45^\circ, -45^\circ, 90^\circ, 90^\circ, 0^\circ\}$  orientations (for more details concerning notation and concepts for Classical Lamination Theory, as well as calculations for the stiffness terms, see Jones<sup>13</sup>). One of the differences that exists between traditional laminates and elastically-tailored ones that employ tow-steered plies is the extra parameters that need to be defined for the variable stiffness plies. In keeping with the standards of Classical Lamination Theory, plies are represented in terms of their orientation angles. For the tow-steered definitions used here, this definition can be limited to  $\phi$ ,  $T_0$ , and  $T_1$ , with the remaining parameters included only if they are different from expected values. Thus, the notation for a tow-steered ply is of the form  $\phi < T_0 | T_1 >$ .

The other major difference between traditional and tow-steered laminates is that the latter possess stiffness matrices that are functions of location. That is, the terms in (2.8) are functions of  $x$  and  $y$ . Due to this complication, several concepts inherent to Classical Lamination Theory must be re-examined.

A *symmetric* laminate is one that possesses a stacking sequence that is symmetric about the middle surface with respect to material properties, ply thicknesses, and orientation angles. This symmetry is advantageous because it removes the coupling between extension and bending so that the  $[B]$  matrix is identically zero, which is often a desirable design feature and also simplifies many analysis techniques. For laminates with constant thickness tow-steered plies (parallel and tow-drop construction methods), the symmetry condition is maintained as long as the corresponding symmetric layers have identical tow-steered ply definitions (which includes the orientation angles as well as the remaining parameters  $\{x_0, y_0\}$  and  $d$ ). However, for laminates that use the overlap construction method, coupling stiffness terms may exist locally even with a symmetric layup definition. This is due to the method used to fabricate the laminate: the plies are initially laid up on a mandrel shaped like the surface of the structure, and subsequent plies are placed over the previous layers. When overlaps are present, this leads to irregular thickness changes within the laminate, though the inner surface remains flat. Therefore, any location that has extra thickness due to an overlap is not symmetric about the middle surface of the laminate, and requires an offset for correct calculation of the stiffness terms. At the present time, these small adjustments have not been incorporated into the stiffness term calculations for the overlap method, instead symmetry will be assumed for laminates with a symmetric stacking sequence. Symmetric

laminates are notated with a subscript <sub>s</sub> appended to the brackets containing the stacking sequence, so that only one-half of the laminate needs to be defined.

*Balanced* laminates are ones for which coupling between in-plane extension and shear is removed ( $A_{16} = A_{26} = 0$ ). Traditionally, this is accomplished by guaranteeing that for every  $+\alpha$  angle ply in the laminate, a corresponding  $-\alpha$  ply with identical thickness and material properties exists. For tow-steered plies, however, balancing is not so easily accomplished due to the variation of the fiber orientation angles. Ideally, a balanced ply would have orientation angles opposite in sign to the angles produced by the curvilinear courses in the original ply for all points, ensuring that the shear-extension coupling is identically zero. However this is not geometrically possible for curvilinear ply paths due to the finite width of the tow placement machine's applicator head. Though shear-extension coupling is not as undesirable as extension-bending coupling, for many structures it is preferred that normal loading does not produce shear deformation, and vice versa. For tow-steered laminates, grouping balanced plies together so that for every  $\phi < T_0 | T_1 >$  ply there is a corresponding  $-\phi < -T_0 | -T_1 >$  layer enforces balancing on a structural level, so that normal and shear force resultants averaged on the laminates edges are not coupled. Therefore, if a rectangular plate with balanced groups of tow-steered plies is loaded under axial compression, the structure as a whole will not undergo shear deformation, though local areas will possess significant shear stresses and strains. Thus, some amount of balancing is possible by grouping plies together that are reflections of each other about the horizontal and/or vertical axes.

To augment this idea further for the specialized case of rectangular laminates, the structural extensional stiffness matrix  $[A^*]$  is introduced. Recall that the traditional extensional stiffness matrix  $[A]$  relates the in-plane stress resultants to the middle surface strain quantities at every point in the laminate. Similarly, the  $[A^*]$  matrix relates the *average* values of these quantities measured at the edges of the structures, which are assumed to remain straight under normal and shear loading. The assumed deformation is shown in Figure 13, where the stress resultants are calculated as the average of the loads on each edge:

$$\begin{aligned} N_x^* &= \frac{1}{2b} \int_{-b/2}^{b/2} [N_x^+(y) + N_x^-(y)] dy & N_y^* &= \frac{1}{2a} \int_{-a/2}^{a/2} [N_y^+(x) + N_y^-(x)] dx \\ N_{xy}^* &= \frac{1}{4b} \int_{-b/2}^{b/2} [N_{xy}^+(y) + N_{xy}^-(y)] dy + \frac{1}{4a} \int_{-a/2}^{a/2} [N_{yx}^+(x) + N_{yx}^-(x)] dx \end{aligned} \quad (2.9)$$

Using these definitions and the straight edge deformation shown in Figure 13, the relations for the structural extensional stiffness matrix  $[A^*]$  are given as

$$\begin{Bmatrix} N_x^* \\ N_y^* \\ N_{xy}^* \end{Bmatrix} = \begin{bmatrix} A_{11}^* & A_{12}^* & A_{16}^* \\ A_{21}^* & A_{22}^* & A_{26}^* \\ A_{61}^* & A_{62}^* & A_{66}^* \end{bmatrix} \begin{Bmatrix} \Xi \\ \Psi \\ \Gamma \end{Bmatrix} \quad (2.10)$$

Note that this matrix is not necessarily symmetric for variable stiffness laminates, though it does reduce to the traditional  $[A]$  matrix for a constant stiffness laminate. The entries in the matrix are most easily calculated by performing an in-plane analysis for each of the displacement quantities  $\{\Xi, \Psi, \Gamma\}$  individually, and can be used to estimate the global stiffness response of the structure. Thus, for a properly balanced tow-steered laminate discussed earlier, the  $A_{16}^*$ ,  $A_{26}^*$ ,  $A_{61}^*$ , and  $A_{62}^*$  terms will be zero.<sup>§</sup>

---

<sup>§</sup> In general, four plies are required for overall balancing of an arbitrary tow-steered ply for a rectangular plate. This is due to the fact that balancing requires a symmetric variation of stiffness about both the  $x$ - and  $y$ -axes. For a tow-steered ply centered at the origin, this can be accomplished using a  $-\phi < -T_0 | -T_1 >$  layer. However, for variations that are not symmetric about the origin due to  $\{x_0, y_0\}$  translations within the ply definition, three plies are needed to properly balance a ply defined by  $\phi < T_0 | T_1 >$  with the variation axis located at  $\{x_0, -y_0\}$ . These three layers consist of a  $-\phi < -T_0 | -T_1 >$  ply centered at  $\{x_0, -y_0\}$ ; a  $\phi < T_0 | T_1 >$  ply at  $\{-x_0, -y_0\}$ ; and another  $-\phi < -T_0 | -T_1 >$  ply at  $\{-x_0, y_0\}$ .

Finally, it should be noted that in practice, laminates that use tow-drop and/or overlap construction techniques require the outer plies to be traditional constant stiffness laminates. This ensures that the external surfaces of the laminate do not possess gaps or overlaps which are more susceptible to degradation. Interspersing different construction techniques within a laminate is also possible, though not considered here.

### 3.0 Implementation of Tow Steering Definitions within *STAGS*

Analysis of structures that utilize tow-steered plies requires a numerical process that can assess the local stacking sequences at each point within the laminate. Earlier research by these authors relied on several different algorithms to estimate the response of elastically tailored rectangular plates. The first method was an in-house Rayleigh-Ritz solution for flat rectangular plates subjected to in-plane loading.<sup>14</sup> This numerical solution technique was intended specifically for the tow-steering definitions outlined here, and the procedure was designed to be numerically efficient so that it could be used in large-scale design and optimization studies. However, for structures beyond the complexity of a simple flat panel, a more rigorous finite element solver was required. Such a tool was developed during the first phase of this research,<sup>6</sup> which consisted of Java-based software that could translate an existing finite element model into one that was defined using the tow-steered definitions. The main drawback of the Laminate Definition Tool software (referred to as *LDT*) was execution time. This led to the present development of an automated finite element analysis technique that could incorporate the tow-steering definitions as before, but do so in an efficient manner that would enable the more accurate solver to be used within the optimization studies. The following sections detail the implementation of this automated solver through the use of *STAGS* (STructural Analysis of General Shells<sup>15</sup>), a finite element solver developed by Lockheed-Martin for general shell structures.

The main advantage of using *STAGS* for this research is that the FORTRAN source code is accessible to the user and is anticipated to be modified for special purpose solutions. In comparison to many commercial finite element packages, this provides an opportunity to bypass some unnecessary details of the solution and streamline the algorithm to only output the parameters necessary for design optimization. Furthermore, conventional definitions of the finite element models are enhanced through user-written subroutines that allow customized input parameters to be employed. This last feature is used here to define the local stacking sequences that arise from the elastically-tailored laminates. Some background on the basic structure of the *STAGS* solver is provided first, to familiarize the reader with the processes involved and identify the modifications required to develop an automated solution algorithm. Details of the user-written subroutine are then provided, and some comparisons to previous solutions using the *LDT* software are included to emphasize the increase in numerical efficiency and accuracy. Note that the discussions in this section assume a working knowledge of finite element methods and the FORTRAN computer language. Further explanation of many of the concepts referred to here can be found in references 15 and 16.

#### 3.1 Finite Element Modeling using *STAGS*

Modeling of shell structures within *STAGS* consists of two basic types. The first uses shell units, which are based on conventional shell geometries (such as rectangular panels, circular cylinders, and cones) and are discretized with respect to a numbering system based on rows and columns that are defined by the user. This provides a concise method to define the geometry of basic geometric shapes. More detailed discretization that does not fit in with the row/column format is accomplished through the second type of geometry definition, termed element units, which are analogous to elements used in most general purpose finite element packages. Elements require a framework of node points to define their position in three-dimensional space, and come in an assortment of types (beams, triangular and quadrilateral shell elements). Node points, as well as locations within shell units, can be constrained with respect to

translation and rotation and can be acted upon by various types of load conditions. Modeling of the continuum is achieved through the definition of shell wall properties, which can be linked to both shell units and elements. The shell properties, in turn, are based on stacking sequence definitions which reference general material properties. All of this input data, along with other output and procedural information, is stored within a text data file, which is identified by a user-supplied *casename* string and the *.inp* suffix. A second text file, designated by *casename.bin*, contains solution control information (such as linear bifurcation of nonlinear analysis). Execution of *STAGS* consists of two phases. The set-up phase *S1* reads in the input file (along with other optional files that may be required if initial geometric imperfections are being considered), verifies the feasibility of the model, and stores information necessary for analysis in a binary file. The *S2* phase uses this binary file along with the solution control information to perform the analysis, which can be stopped, restarted, or executed again without executing the *S1* phase. Analysis results are stored in a variety of text and binary files, which can be post-processed to extract the desired performance measurements.

For this research, attention is focused on the designation of the stacking sequence for models defined using traditional element units.<sup>\*\*</sup> Each element is defined in terms of the nodes that it is connected to as well as its type and a reference to the associated shell wall properties (or cross-sectional properties for beam elements) which are supplied elsewhere within the text file. For a traditional constant stiffness laminate, a single shell wall property can be defined and referenced by each element to provide a unique stacking sequence for the entire structure. For an elastically-tailored laminate utilizing tow-steering concepts, each element must be assigned a unique stacking sequence according to the location of the element centroid. This process often amounts to a significant degree of effort, and led to the development of the Laminate Definition Tool<sup>6</sup> which performs this task automatically for a pre-existing input file. However, there were several drawbacks to this re-definition method. In the first place, the considerable input/output time associated with reading in the model, calculating the locally varying stacking sequences according to the chosen laminate definition, and rewriting a new input file made it impossible to use within a design environment. Secondly, the resulting input file was hard-wired for the specific tow-steered laminate definition, and required execution of the *S1* phase for each new definition even though the only modification to the file was the designation of the individual element stacking sequences. Lastly, basing the shell wall properties on a calculation at the element centroid resulted in the finite element solver assuming a constant stiffness variation within each individual element, thereby ignoring the local stiffness variation present within the domain of the element. This omission may affect accuracy and convergence, since it effectively averages the stiffness distribution over the element which leads to slightly erroneous estimates of the local stiffness parameters.

The disadvantages of the re-definition method are rectified through the use of the *WALL* subroutine, which is a user-written subroutine provided with *STAGS* that is intended to be used for structures that have variations within the shell wall property definition. Thus, instead of a hard-wired definition of the stacking sequence for each element, the parameters of the subroutine can be used to provide the relevant data to the finite element solver in a function call manner. This alleviates the problem of input/output time associated with writing stacking sequences, since the layup data is never converted to text form. Within the input file, the indicator for when to use the *WALL* subroutine is contained in the element definition in place of the reference to the hard-wired shell wall properties (more specifically, the *IWALL* parameter). Shell wall properties that are designated in this manner are interpreted by the *S1* set-up phase as run-time quantities, which are calculated during the *S2* analysis phase. Therefore, more efficient use is made of execution time. The set-up phase is only required to be executed once for each model/input file, and subsequent designs that differ only in stacking sequence designation can be analyzed with independent execution of the *S2* analyzer. Lastly, as will be shown in Section 3.2, the implementation of the *WALL*

---

<sup>\*\*</sup> The method outlined here for element units is easily extended to *STAGS*' shell units. The modifications required for shell units that utilize tow-steered definitions are discussed within the text of Section 3.2.

subroutine ensures that stacking sequence calculations will be requested at the integration points within each element, as opposed to the element centroid, which provides a more accurate modeling of the gradual stiffness variation produced by tow-steering methods. Comparisons to the original re-definition technique are provided in Section 3.3 to substantiate this claim.

### 3.2 Stacking Sequence Designation using the WALL Subroutine

The WALL subroutine is called within *STAGS* whenever wall property information is required. This occurs most often during the construction of the global stiffness matrix, which is built up from local stiffness parameters calculated at the integration points of each element. For shells constructed with multiple layers, the local stiffnesses are represented in terms of stacking sequences, which are stored within the code using COMMON blocks. The task of the subroutine is to supply this stacking sequence information for the elements and/or shell units that have been designated to reference it. The calling sequence of the WALL subroutine within the *STAGS* code is structured as

```
subroutine WALL(iunit,ielt,kelt,XYZg(3),XYs(2),zeta,ecz,ilin,iplas). (3.1)
```

The first three parameters are integers which indicate the shell unit number, element unit number, and element type, respectively. XYZg and XYs are real-valued arrays (dimension indicated by the number in parentheses) which are the important input parameters for our purposes. XYZg represents the three-dimensional global coordinates of the integration point, while XYs is used for shell units only and symbolizes the surface coordinates. *STAGS*' surface coordinates are defined in a similar manner to the fabrication coordinates discussed in Section 2.2.1, so that implementation of the tow-steering definitions for shell units is quite straightforward. For models constructed using element units, which are used exclusively here, the three-dimensional global coordinates must be converted to fabrication coordinates depending on the geometry of the structure. Note that this transformation must be supplied by the user and hard-wired into the coding. For example, a flat panel situated in the XY-plane would simply use the first two elements of the XYZg array for the fabrication coordinates. Other geometries or flat panels positioned differently would require the necessary transformation from global to fabrication coordinates, as discussed in Section 2.2.1. Thus, it is necessary for coding to be included to ensure that the point under consideration is correctly transformed into the fabrication coordinates that are used by the tow-steered ply definitions. The four remaining parameters in (3.1) are output parameters which are assigned within the subroutine and dependent on the problem under study. They represent respectively a local rotation within the element used to reference the fiber orientation angles; the eccentricity of the wall properties with respect to the middle surface<sup>††</sup>; and two integers indicating linear/nonlinear strain-displacement relations and elastic/plastic material response. It will be assumed here that these final four parameters are accounted for by the user and designated accordingly within the user-written subroutine.

The main parameters within the COMMON blocks that need to be supplied include the type of wall configuration (a layered wall for composite laminates), the number of total layers, and the material identification, thickness, and orientation angle of each angle. These last four parameters represent the stacking sequence and are calculated for the given point in fabrication parameters from a tow-steering module written for this purpose, based on the equations presented in Section 2.2. The layup definition is designated within a special input file that is read by the tow-steering module, named *casename.tsl*, which contains the stacking sequence information in NAMELIST format.<sup>16</sup> An example input file using the appropriate input parameters is shown below:

---

<sup>††</sup> This eccentricity parameter would serve as the necessary offset adjustment for laminates that use the overlap method as discussed in Section 6, however it has not been implemented as yet.



```

&LAYUP_PARAMETERS nplies=6 symmetric=true/
&PLY_DATA matlID=1 t=0.0054 phi=45.0/
&PLY_DATA matlID=2 t=0.0054 method='TowDrop' phi=0.0
    t0=45.0 t1=60.0 loc=7.5/
&PLY_DATA matlID=1 t=0.0075 method='Overlap' x0=2.0 phi=90.0
    t0=-45.0 t1=0.0 loc=7.5/

```

(3.2)

NAMelist format requires that each dataset is named and preceded by an ampersand(&), and the data should end with a slash(/). The first dataset in the input file contains an integer designating the number of total plies in the laminate, plus a boolean indicator signifying if the layup is symmetric or not. If symmetric, only one-half of the entire number of plies need be defined, the rest are automatically calculated within the module. The following lines contain the individual ply definitions. Each set of ply data must contain a materialID designation, which should correspond to material data within the STAGS input file, and a ply thickness parameter  $t$ . Both of these parameters are required. The rest of the parameters are optional according to the characteristics of the ply, and have default values if the parameter keyword is not supplied in the definition. Specifics of each parameter are given below.

method={'Constant', 'Parallel', 'TowDrop', or 'Overlap'}. This parameter determines which construction method is being used. The default value is 'Constant'.

refPath={'linearAngle' or 'circularArc'}. Determines the basis of the reference path. The default value is 'linearAngle', the only value used during this investigation.

x0=[real number], y0=[real number]. Origin of variation. Both are defaulted to zero, so that only non-zero values need be specified.

phi=[real number]. Major direction of stiffness variation. For constant stiffness plies, phi is the value of the fiber orientation angle. The default is zero for tow-steered plies.

t0=[real number]. Angle at origin (in degrees) for a tow-steered definition. Required for a tow-steered ply.

loc=[real number]. Characteristic distance for a tow-steered definition, given as  $d$  in equations (2.4) through (2.7). Required for a tow-steered ply.

t1=[real number]. Angle at distance loc (in degrees) for a tow-steered definition. Required for a tow-steered ply.

overlap=[real number]. This parameter determines the amount of overlap between successive courses when the overlap method is used. Its value, along with the angle designations, is used to calculate the shift perpendicular to the  $\phi$ -direction for a new course. The default value is 1.0, which produces a ply with no gaps which overlaps at certain regions along the path. A value of 0.0 gives no overlaps but significant gaps between courses. Values greater than 1.0 produce increasing overlaps proportional to the value of the head width.

head=[real number]. Width of the tow placement machine applicator head. Used for a tow-drop or overlap ply to determine the shift parameter. Default is 3.0 (inches). Large values of this parameter produce an equivalent parallel method ply, while extremely small values used with the tow-drop method produce a stiffness variation that is wholly unidirectional.

Any errors in these parameters, including infeasible plies that contain a center of curvature, are reported to the casename.out2 result file, which is automatically generated when the s2 analysis phase is executed. Different methods can be intermixed for a given laminate. In practice, this is regularly done for

laminates that use the tow-drop and overlap methods. The outer surface plies (top and bottom of the laminate) are designated to be constant stiffness plies so that the gaps and/or overlaps that occur for the tow-steered plies are effectively covered by the constant stiffness plies. Also note that traditional constant stiffness laminates can be easily defined using only the constant angle ply method. This allows for a laminated structure to be analyzed with different layups without altering the input file, which is useful for traditional stacking sequence design or conducting parameter studies to compare the performance of different layups.

### 3.3 Comparisons to Previous Finite Element Solutions

To illustrate the efficiency of this technique and verify the solution, comparisons to models using tow-steered plies that are defined using hard-wired stacking sequences for each element (produced using the *LDT* software) were conducted. Since the hard-wired models evaluate the stacking sequences only at the center of each element, some information regarding the variation of the stiffness is inevitably lost. Alternatively, the use of the *WALL* subroutine directs stacking sequence calculations to be performed multiple times for each element at the integration points, and the variation of the stiffness is more accurately approximated through the interpolation functions of the element. Furthermore, since plies made with the overlap construction method contains small wedges of extra thickness within the overlap region, the analysis requires a denser mesh of points for accurate modeling. Numerical results demonstrating this point are displayed in Figure 14, and are based on a model of a rectangular panel with varying mesh densities to isolate the effect of the size of the elements on the variable stiffness solutions. The abscissa represents the logarithm of the number of nodes in the model, while the ordinate reflects the eigenvalue for the rectangular panel under axial compression. Note how the *LDT* results oscillate more dramatically for the coarser meshes, and have not yet converged to the more accurate solution even for the densest mesh. The *WALL* subroutine solution, on the other hand, quickly converges to a correct eigenvalue with little fluctuation, indicating a more stable algorithm.

Besides the improvement in accuracy for models of the same size, the user-written subroutine increases the efficiency of the solution method since the input/output does not need to be performed. A breakdown of the execution times including the translation time of the model for a tow-steered laminate using the *LDT* method, the set-up time for the *S1* phase, the *S2* analysis phase, and the total time from start to finish is shown in Figure 15 for the same models of a rectangular panel constructed with the overlap method. The translation phase corresponds to the execution of the *LDT* software, which hard-wires the stacking sequences for each element in the model. Thus the set-up time *s1* is larger for the *LDT* models because a stacking sequence must be read in for each element, but the analysis time is shorter since the data is readily available for the *s2* solution phase. As expected, the total time is much lower for the user-written subroutine technique (note that the ordinate uses a logarithmic scale, which tends to diminish the large differences between values). Re-analysis time for multiple stacking sequence designs corresponds to the total time for the *LDT* method (since each model must be defined from scratch), yet is equivalent to the *S2* analysis time only for the *WALL* subroutine technique. The significant savings suggest the suitability of the new method for optimization and design studies, which are the topic of the following sections.

## 4.0 Laminate Design using *OLGA*

The suitability of the tow-steered definition for stacking sequence optimization was an original goal of the parameterization. Previously, large-scale design studies relied on a numerically efficient solver to analyze the performance of the various laminate layups,<sup>14,17</sup> however the availability of the general finite element solver *STAGS* as an automated analysis tool has created the possibility of using more complex solution techniques within the design process. This chapter details the integration of the finite element solver with *OLGA* (Optimization of Laminates using Genetic Algorithms), a stacking sequence optimization

environment developed by ADOPTTECH to design monolithic and sandwich composite panels using tow-steering and blending design concepts. The first section provides basic background to familiarize the reader with the framework of the design software. Modifications performed to implement the *STAGS* solver within the design environment are then detailed, including the method used to automate the analysis process and new dialogs within the software that are used to specify the configuration of the finite element model that is being designed.

## 4.1 Structure of Design Environment

*OLGA* is a graphical user interface based on the Java<sup>18</sup> programming language that is used to design composite laminates with the aid of Genetic Algorithms.<sup>19</sup> Genetic Algorithms are atypical when compared to classical optimization schemes in that derivative information for objective functions and constraints are not required, thereby making the algorithm well-suited for optimization problems that utilize discrete-valued design variables, such as ply angles and material choices for stacking sequence design. This section illustrates the organization of the *OLGA* software and introduces some of its advanced features which pertain to the design of tow-steered laminates. Provisions for incorporating *STAGS* as part of *OLGA*'s composite laminate analysis toolbox are detailed in Section 4.2.1.

### 4.1.1 Specification of Design Problem

The main dialog presented when *OLGA* begins execution is shown in Figure 16. The menu items and buttons located along the top of the dialog dictate the operation of the software. Two of the menus are self-explanatory, such as the **File** menu which controls the loading and saving of various optimization runs and the **Help** menu. The **Mode** menu determines the analysis technique used by the optimizer, being either the included numerical solution for flat panels or an external finite element solver, and will be discussed in more detail in Section 4.2.1. For the present discussion, we will assume that the *Panel* mode has been selected, which is the default value for the software. The **Specification** menu is used to define the design problem under study, and will be discussed in detail shortly. The **Database** menu provides access to information for the composite and core materials that may be used within the design process, and the **Options** menu provides controls for modifying the Genetic Algorithm's optimization parameters. The remaining menu, **Plots**, is used to graphically display results of the design run and will be discussed in the next section. The rest of the main dialog consists of buttons to control the execution of the design process; a large text area that displays the status of the optimization run and provides ongoing and final results; and status information at the bottom of the console which monitor the important parameters during the optimization run. The use of this information will be made more clear in the next section, when an execution example is provided.

Returning to the **Specification** dialog, each menu item in the list opens a corresponding dialog that is used to specify parameters associated with the design problem. Note that when *OLGA* is initialized or a previously saved configuration is loaded, each of these dialogs will contain default information so that specifying each set of data is not always required. The following paragraphs summarize the operation of each dialog and indicate the possible options that exist for the design of composite laminates.

Panel Configuration Dialog (Figure 17): This dialog is displayed when the **Configuration** menu item is selected from the main **Specification** menu and the **Mode** is set to *Panel*. Parameters for a grid of monolithic and/or sandwich panels are prescribed here. Initially only one panel is present, and the parameters at right are used to specify if the panel is monolithic or sandwich, the dimensions and position of the panel, core characteristics if the panel uses sandwich construction, and panel loading parameters. Note that the loading parameters represent average edge loads in accordance with the quantities defined in (2.9). Additional panels are generated by altering the number of panels in each direction and selecting the *Layout Panels* button. Specifications for each panel are displayed by selecting the appropriate panel number from the drop-down box in the upper right of the dialog. Each panel can have independent

specifications and can also be excluded from the design problem through de-activation. An example of six panels (one de-activated and selected not to be displayed) is shown in the layout area on the left. Multiple panel configurations are used for blending (discussed later) or to design panels with different geometric, response, and/or loading characteristics simultaneously.

Fabrication Dialog (Figure 18): Options regarding the construction method used for the laminates are defined here. If *Straight Fiber* is selected, the entire grid of panels are designed using standard stacking sequence optimization based on the constant fiber orientation angle of each layer. Conversely, *Steered Fiber* allows the use of curvilinear fiber formats within the design process, as described by the parameters in Section 2.0. Parallel, tow-drop and overlap methods, as well as the pointwise method which is a construction technique associated most with blended laminate design, can be selected for the design process. The tow-steering definition parameters are also selected within this dialog, including the origin, direction and characteristic distance of the stiffness variation. A linear variation of the orientation angle is the default for the reference curve function, though other options are available and new definitions can be integrated quite easily. Shortcuts exist for the most common configurations (*Horizontal/Vertical* and *Centered*), where the tow-steering parameters are calculated automatically according to the limits of the panel grid in the *Panel Configuration* dialog. Alternatively, exact values of the tow-steering parameters can be specified using the *User-defined* option. Note that the fabrication method selected applies to the entire panel grid and cannot be selected individually for each panel. Finally, the bottom section of the dialog provides parameters concerning the manufacturability of a tow-steered ply. Minimum radius of curvature and the head width need to be provided (the head width being the number of tows multiplied by the individual tow width, assumed to be 24 tows of 1/8 inch width as the default), while the cut length parameter is only required when tow-drop courses are generated to check for manufacturing feasibility (not part of the design process). These parameters are not required when *Straight Fiber* design is selected.

Responses Dialog (Figure 19): Objective function and constraint information are specified in this dialog, which operates on a panel-by-panel basis for multiple panel configurations through the drop-down box. Either cost or weight can be chosen as the objective function to be minimized, and the option also exists for multi-objective optimization (though this must apply to all panels). Strength and stability constraints can be selected for each panel (buckling selection is checked to ensure that instability is possible for the given loading conditions), and several sandwich panel constraints are also available if the panel is of sandwich construction. Constraints are evaluated by the analysis tool based on the panel load levels, and designs that fail below these levels add a penalty to the objective function. A small bonus is awarded to designs that do not violate a constraint. The bonus parameter is based on the constraint with the most critical safety factor (i.e., the constraint closest to violation), and allows the genetic algorithm to differentiate between designs of equal weight or cost. This favors designs that are most able to withstand the applied loads yet does not detract from the more important design objective.

Layup Definition Dialog (Figure 20): The layup definition dialog contains the pertinent details for the construction of the laminate stacking sequence. The uppermost section prescribes the global aspects of the layup, including if the laminate is symmetric (always the case at the present time), the number of layers (which can be fixed, or given and a minimum and maximum value), minimum and maximum thickness of the laminate, and a constraint on the maximum number of contiguous plies. Balancing<sup>††</sup> is accounted for in several ways. One option is for the laminate to be unbalanced, resulting in the possibility of stacking sequences that contain extensional-shear coupling. Alternatively, balancing can be enforced through the operation of the Genetic Algorithm, which contains logic that tries to balance laminates automatically and rewards the balanced designs. Balancing can also be identically satisfied by using two-ply stacks, consisting of a  $\pm\theta$  group for off-axis plies ( $\phi \pm \langle T_0 | T_1 \rangle$  plies for a tow-steered laminate) and two-ply groups for  $0^\circ$  and  $90^\circ$  plies. A drop-down box also exists to specify the configuration of a stacking sequence that utilizes tow-steered plies. Each layer can be defined by any tow-steered ply configuration or

---

<sup>††</sup> Balanced here implies that the laminate is balanced in a structural sense, as discussed in Section 2.3.

the outer plies can be constrained to remain constant, which protects the gaps and overlaps from external degradation. The middle section of the dialog governs the particular angles that are available to the designer. Maximum and minimum limits can be applied if required for certain manufacturing constraints. The angle choices are limited to increments of  $15^\circ$ , and represent the possible values of  $\theta$  for constant stiffness plies and  $T_0$  and  $T_1$  for tow-steered definitions. The lowermost section identifies which materials are available for the stacking sequence designs. Material information is stored in the material database (not shown) and includes stiffness and strength parameters as well as ply thickness, density, and cost. Multiple materials can be selected for both the laminate and the sandwich core, where applicable.

**Blending Dialog** (not shown): The remaining item under the **Specification** menu is for blending. This dialog is intended for multi-panel designs and offers several strategies for blending the layups between adjacent panels. Blending implies that the disparate stacking sequences that arise from the optimization of each panel are altered to give the best performance for the panel structure as a whole while enabling more efficient fabrication. This can be accomplished by stipulating that each panel must use the same laminate, or that they share common layers within their layups. Since blending is not presently an option for finite element-based analysis, further details will not be furnished here though some examples are available as a reference.<sup>17</sup>

#### 4.1.2 Execution of Optimization Run

Once the specification of the problem is complete, execution begins by pressing the *Start* button in the main dialog (see Figure 21). This initiates the optimization run, whose first step is to write an input file for *DARWIN*, the Genetic Algorithm that controls the design process. The *DARWIN* program is coded in Fortran90, operates externally to the *OLGA* software, and communicates with it through data streams and input/output files. In general, the input file defines the discrete valued design variables that are used by *DARWIN*, including the angle combinations and material choices specified in the Layup Definition dialog. For tow-steered laminates, the feasibility of the tow-steered configurations are estimated first. All combinations of  $T_0$  and  $T_1$  are input to the analysis module for each panel, and the calculated minimum radius is compared to the allowable limit due to the manufacturing constraints. If the  $\phi < T_0/T_1 >$  combination is manufacturable given the allowable constraints, it is assigned a distinct integer value and added to the set of design choices that is written to the input file. Note that this calculation is accomplished by the analysis module without requiring a full static or buckling solution, so that the minimum radius calculation can be performed quickly. The information console within the main dialog reports the angle combinations that are used, as shown in the top pane of Figure 21, as well as the available material choices.

*DARWIN* uses the input file information to begin the optimization process. The genetic algorithm procedure is initialized by generating a random population of laminate designs. Each design is analyzed and assigned a fitness value according to the calculations for the objective function and constraint values. Succeeding populations are formed by applying various probabilistic operators that recombine existing members of the population. Members in the population with higher fitness values have a greater probability of being eligible for parenting the next generation. Generations continue to be produced and the highest ranked members monitored until the optimization run is completed, which is either based on a fixed number of total generations or a completed number of generations without improvement in the best design found by *OLGA*. Run time parameters are monitored by the *OLGA* software at the bottom of the main window, and the *Update* button displays the best designs at a given point in the optimization run. An update instance is shown in the bottom pane of Figure 21. The laminate design is displayed with its individual angle definitions and material choices decoded from the internal string combinations, and the objective function and constraint values are also provided. *DARWIN* stores information for a predetermined number of designs, and more detailed results for the highest ranked designs can be produced using the drop-down box above the main information console. The **Plots** menu also contains graphical results of the design run, including optimization history and pareto plots for multi-objective

design. Thus the final results of the optimization run provide a set of manufacturable layups with the lowest weight and/or cost that best satisfy the loading constraints.

## 4.2 Implementation of *STAGS* Solver

Integrating a general finite element solver within the design environment of *OLGA* presents some obstacles. However, there exists a need to be able to analyze more complex elastically-tailored structures so that the full potential of the tow-steering concept can be investigated. Fortunately, the capability of *STAGS*' user-written subroutines enable accurate modeling of the tow-steered designs for many shell structures. This section details the modifications required to incorporate a *STAGS* analysis capability into *OLGA*, including new dialogs in the software to specify the design problem and the technique used to automate the analysis run. Future modifications to address known shortcomings and enhance the capabilities even further are also furnished.

### 4.2.1 Finite Element Model Interface Dialog

When finite element models are used for structural analysis, the *STAGS* solver (which employs the *WALL* user-written subroutine as outlined in Section 3.0) is used in place of *OLGA*'s default panel analysis code. A new design mode was implemented within *OLGA* to reflect this change. *Panels* mode, signified by the highlighted box in Figure 21, uses the existing panel analysis solver for panel grids represented by Figure 17. *FE Model* mode (chosen through the **Mode** menu or button selection) obviates the use of the panel configuration dialog and produces a finite element model interface dialog when the configuration menu item is selected for specification. Presently, only one finite element model can be designed at one time, preventing some of *OLGA*'s advanced features, such as blending, from being used. However, the remaining specification dialogs introduced in Section 4.1.1 all operate as before, with a few exceptions that are discussed forthwith.

The finite element model interface dialog is shown in Figure 22, where an existing *STAGS* model has already been imported. Most *STAGS* models using basic shell units and elements can be read in by the software, except for some advanced features that have not been implemented until required. Errors in the input deck are reported to the console, and a valid solution control file (see Section 3.1) must also exist so that proper execution of *STAGS* can occur.<sup>§§</sup> Furthermore, the geometry specification must not reference a different *WALL* user-written subroutine, since that is the method used to introduce the design variables. A valid model is displayed in the finite element model interface dialog in its own coordinate system, where the transformation to fabrication coordinates (discussed in Section 3.2) should be satisfied by the user within the *WALL* subroutine. A rectangular bounding box that defines the coordinate limits of the model is also calculated during the import process, which is used to locate the variation definition and estimate the maximum curvature manufacturing constraint. Element and node information is available within the dialog, as shown by the pop-up in Figure 22. This enables the user to double-check the integrity of the model and correctly choose the elements desired for design. Translations, close-ups, and rotations of the model can also be performed through typical graphical user interface methods to provide comprehensive views of the model.

Elements selected for design are signified by the gray elements in Figure 22. Element selection is performed through mouse operations and/or keystrokes. Any unselected elements maintain their laminate definition as specified in the model input file, while the selected elements reference the *WALL* subroutine and their stacking sequences are calculated at run-time. A new model input file, reflecting these changes to the selected elements (and including any new materials that may have been selected for stacking

---

<sup>§§</sup> Presently, only linear bifurcation analysis has been implemented for structural failure within *STAGS*, therefore an *analyze.bin* file set-up for linear buckling analysis is the default solution control file. Further details on the analysis capabilities of *STAGS* within the design environment are discussed in Section 4.2.3.

sequence optimization) is written to a `analyze.inp` file through the *Write File* action once the element selection is complete. Also note the circle and solid line in Figure 22 (magenta if viewed in color), which represents the origin, direction, and characteristic distance of the stiffness variation when tow-steered definitions are specified in the fabrication dialog (Figure 18). Though not required to create the new model input file, this device is useful to validate that the correct stiffness variation is being used by the design software, and is automatically updated for new models and geometries.

#### 4.2.2 Automated STAGS Execution

Once a proper model input file is re-written and the remaining design specifications are completed, *OLGA* is ready to begin the optimization run. The first step, as before, is to determine which tow-steered angle combinations are feasible for the geometry under consideration. This is performed using the included panel analysis model (since it is much faster) based on the rectangular bounding box calculated during the model import process. Secondly, the model input file is prepared through execution of the *S1* set-up phase of *STAGS*. This need only be performed once during the entire optimization run, and sends an error to the console if the input file is not valid.

The optimization run continues as *DARWIN* constructs the design population. Analysis is performed for each design through external stream commands and temporary data files. The first step is to translate the design string generated by *DARWIN* into a tow-steered definition written in NAMELIST format, such as the data in (3.2). This data is written to a file called `analyze.ts1`, which is read by the *WALL* subroutine during the analysis phase. Execution of a customized *S2\_olga* analysis program performs the finite element calculations and writes specific model information (weight, cost, buckling eigenvalue, and/or material failure safety factor) to a temporary file titled `analyze.olgaOut`. This streamlines much of the input/output associated with *STAGS*: all of the standard output features are minimized, and the necessary information is written directly to a small file that is easily input to the design software. Subsequent designs merely need to re-define the `analyze.ts1` file and execute the *S2\_olga* analysis program. Duplicated designs are not re-analyzed, since each member of the design population is automatically stored in a binary tree within *OLGA* to save on computation time.

Final results are identical to those displayed in Figure 21, and re-analysis is accomplished through the use of the existing `analyze.inp` file and a correctly defined `analyze.ts1` file. Therefore, detailed post-processing of the best designs is easily performed to explore the mechanisms behind the performance improvements and visualize the results. Examples of this design method are provided in the following chapter.

#### 4.2.3 Future Modifications

The procedure outlined here for stacking sequence and tow-steered design using *STAGS* is the first step towards an automated design environment using finite element analysis. Though the techniques developed under this task satisfy the requirements outlined for this research and provide useful tools for laminate design, several enhancements and improvements have been discovered during this phase. This section describes several of the features that either need improvement from the present state or show great promise for future tasks.

- First-ply-failure failure and laminate degradation techniques, that are available in *STAGS* through the GCP data format, are not presently configured to work with laminates defined using the *WALL* subroutine. Therefore material failure constraints cannot be evaluated within the design process at this time. An update to *STAGS* to rectify this problem is under development, but was not available before the end of this project. Once rectified, it is hopeful that limit load designs utilizing post-buckling and progressive failure analysis can be performed, though analysis time may be a limiting factor.

- Presently, design of a laminate within a finite element model is limited to one stacking sequence for the selected elements within the model. In the future, designation of several design zones within one model (or simultaneous design of independent models) that would utilize the blending features of the design software would be extremely beneficial. For example, a structure that is constructed of four connected sub-components could be analyzed with independent or blended stacking sequences that account for the manufacturing techniques used for the structure during the design process. This technique would mirror the multi-panel capability of the *OLGA* software that is available in *Panels* mode.
- Local eccentricity of tow-steered laminates that utilize the overlap construction method needs to be incorporated within the stacking sequence definition. Though this slight error should not significantly affect the design results, inclusion of this feature should provide better agreement to test results and possibly shed light on other undesirable manufacturing defects, such as local imperfections of a laminate due to post-cure curvatures.
- The possibility to intersperse different construction techniques and variation directions within a single laminate must be introduced. Though a simple technique was developed here to accommodate variations in mutually orthogonal directions (see the results of Section 5.3), more general choices should be available to fully explore the potential of these elastic tailoring methods.
- Sandwich panel construction must be available for *FE Model* mode, and specific failure criteria developed exclusively for sandwich laminates must be estimated by the *STAGS* solver. Additionally, cost is not a standard parameter for materials within *STAGS*, so that ad hoc methods are presently used to estimate laminate cost during the analysis phase. An automatic estimation of cost within *STAGS* is preferred.
- The finite element model interface dialog could be expanded to perform more complex tasks. This could include importing models that use different finite element packages and re-writing in *STAGS* format for subsequent design, or rudimentary model generation within the graphical user interface. Calculation of tow paths for selected designs overlaid directly onto the model surface could also be useful for visualization of the prototype designs.
- Keywords in the `casename.tsl` file should be configured to designate model geometries within the *WALL* subroutine. This is helpful to correctly identify which transformation to invoke between the model coordinates and the surface coordinates used by the tow-steered ply definitions.

## 5.0 Design Examples

This chapter presents the results for several design examples involving buckling of flat plates. The first two problems are based on earlier design results generated by these authors during earlier phases of this task,<sup>6</sup> and demonstrate the effectiveness of the *STAGS* solver as the analysis tool during the design process. The final design problem investigates the use of curvilinear fibers for a square plate with a central hole subjected to shear loading. All studies employ a standard graphite-epoxy material for each lamina, with material properties given in Table 1 below.

**Table 1: Material Properties for AS4/9773 Composite System**

| Longitudinal Modulus, $E_1$ | Transverse Modulus, $E_2$ | Shear Modulus, $G_{12}$ | Poisson's Ratio, $\nu_{12}$ | Density, $\rho$           | Ply thickness, $t$ |
|-----------------------------|---------------------------|-------------------------|-----------------------------|---------------------------|--------------------|
| 18.83 Msi                   | 1.34 Msi                  | 0.74 Msi                | 0.36                        | 0.058 lbs/in <sup>3</sup> | 0.0075"            |

These properties conform to the ones used in earlier design studies.<sup>6</sup>



## 5.1 Simply-Supported Plate under In-plane Compressive Load

The panel analysis tool that is the standard solver used by *OLGA* is limited to flat rectangular geometries with simple support edge conditions and no interior holes or cutouts. While these restrictions do not hinder useful panel design, the ability of the finite element solver to model any geometry or boundary condition is a vast improvement for the design technique. However, the trade-off occurs in execution time, where the more robust finite element solver cannot compete with the faster Rayleigh-Ritz panel analysis. Therefore, the first design study employs a finite element model with identical dimensions and boundary conditions to the panel analysis geometry, so that comparable design runs can be investigated to evaluate execution time and design run results. This example also served as a useful test case for the integration of *STAGS* within the *OLGA* design environment.

The *STAGS* model used for this design example is shown in Figure 23. It consists of a flat rectangular plate, measuring 20 inches high and 15 inches wide, with simply-supported boundary conditions on all edges. Elements measure one half-inch square, which leads to a regular mesh of sufficient density to accurately model the stiffness variation (determined by an independent parameter study). Loading is introduced through a vertical compressive load on the top edge of the panel, and all edges are constrained to remain straight. Buckling was the critical constraint for each case. Each design run used 20 members in the population and was stopped after 25 generations, which allows for a maximum of 500 different designs to be generated. Both of these parameters are actually smaller than what would be used for a faster analysis, however results indicate that the design space was adequately surveyed under these limits. Ply angles were chosen from a set of orientation angles in fifteen degree increments, and two-ply stacks were used to ensure balanced laminates. Since the panel analysis is presently unable to perform adequate analysis of the overlap method, only straight fiber panels and the tow-drop method were used for the construction methods. Tow-drop panels had an extra constraint that the external plies had to be straight fiber plies. The results for the four cases, varying the solver used and the construction method, are displayed in Table 2, where *RR* indicates the Rayleigh-Ritz panel analysis solver.

**Table 2: Design Results for Simply-Supported Panel**

| Analysis     | Construction Method | Layup   | Buckling Load (lbs) | Time <sup>***</sup> (sec) |
|--------------|---------------------|---|---------------------|---------------------------|
| <i>RR</i>    | Straight            | $[\pm 45_2/\pm 30/\pm 45/\pm 30]_s$                   | 7918                | 11                        |
| <i>STAGS</i> | Straight            | $[\pm 45_2/\pm 30/\pm 45_2]_s$                        | 7912                | 5438                      |
| <i>RR</i>    | Tow-drop            | $[\pm 45/0\pm <45 60>_2/0\pm <30 15>_2]_s$            | 9326                | 1812                      |
| <i>STAGS</i> | Tow-drop            | $[\pm 45/0\pm <30 45>/0\pm <45 60>_2/0\pm <30 15>]_s$ | 9287                | 9891                      |

For the straight fiber cases, the best designs found using each solver were nearly identical with similar buckling loads. The slight differences exist due to the disparity between the numerical solvers. For example, *STAGS* analysis of the best layup from the Rayleigh-Ritz results (the  $[\pm 45_2/\pm 30/\pm 45/\pm 30]_s$  laminate) produces a buckling load estimate of 7911 lbs, slightly below the best layup found from *STAGS*. Meanwhile the panel analysis solver estimated the buckling load for the  $[\pm 45_2/\pm 30/\pm 45_2]_s$  layup as 7916 lbs. Investigation of the optimization history indicates that both of these layups were evaluated by both solvers during the design run. More extreme disparities occur for the tow-drop construction method. The mesh density of the finite element model produces a more accurate representation of the stiffness variation due to the tow-steered plies than the Rayleigh-Ritz technique, thereby producing greater discrepancy between analysis results. *STAGS* analysis of the best Rayleigh-Ritz design produces a 8794 lbs buckling load, while the panel analysis estimates buckling at 9191 lbs for the best *STAGS* design. Better agreement between the analysis alternatives can be achieved by increasing the number of terms in

<sup>\*\*\*</sup> These analysis times are based on results from a desktop PC running at 400 MHz using a Pentium II<sup>®</sup> processor.

the Rayleigh-Ritz approximation, though this decreases the numerical efficiency of the algorithm. In general, however, the results for the top five designs found by each analysis technique are quite similar, so that re-analysis of a small number of laminates using the more accurate finite element method yields the same ordering of the best designs.

With regard to execution times, the results reaffirm the disparity between the numerical speed of the two analysis techniques. For the Rayleigh-Ritz method, analysis of constant stiffness laminates occurs within a fraction of a second, whereas variable stiffness laminates require additional time for fiber orientation angle calculations and the solution of the in-plane stress resultants. *STAGS* uses the same solution technique for both the constant and variable stiffness laminates, so that the extra time associated with the tow-drop method is attributed solely to fiber orientation angle calculations (four calculations are conducted for each element within a design). As expected, the time savings for the Rayleigh-Ritz technique is quite significant compared to the finite element analysis. Therefore, if a problem is able to be adequately modeled by a set of simply-supported panels, the use of the faster Rayleigh-Ritz technique is preferred.

## 5.2 Rectangular Plate with Central Hole under In-plane Compressive Load

This design problem was the basis of earlier research<sup>6</sup> to prove the worth of tow-steering design concepts. In the previous work, the Rayleigh-Ritz analysis procedure was used in conjunction with the *OLGA* design software to produce a small number of candidate designs, which were then transformed into finite element models and analyzed using *STAGS* to determine which prototype designs to build and test. The results prompted an investigation into the feasibility of using *STAGS* as the analysis procedure within the design process, the major topic of this research. Comparisons are made to the earlier results here, so that the advantages of using the *STAGS* solver are evident.

The design problem is based on a rectangular panel under in-plane end shortening subjected to boundary conditions resulting from experimental testing. A circular hole is located at the center of the panel, which is of two different sizes or absent altogether. The mesh configuration used for the optimization runs is shown in Figure 24, which illustrates both the large and small hole sizes by different shading of the mesh. For the panel without a hole, a regular grid comprises the central region. The gray shaded areas at the top and bottom of the mesh represent the potting of the specimen that is required for testing. Zero displacement and rotations (except for vertical movement) are enforced within this potting region, and the top and bottom edges are constrained to remain straight under a vertical compressive load. The vertical edges are limited by knife-edge supports along the node lines located one quarter-inch in from each edge. The density of the mesh was determined by parameter studies intended to estimate the minimum number of elements needed to accurately model the stiffness and stress variation without requiring excessive computation time.

Results for the panel without a central hole are shown in Table 3 for both the original design technique that used the Rayleigh-Ritz solver along with the Laminate Definition Tool as well as the present *STAGS* solution. Relative increases with respect to the earlier design results are also tabulated. Note that the *RR/LDT* analysis method was hindered in two ways: the boundary conditions of the panel analysis were simply supported on all edges, so that the exact boundary conditions were not considered during the optimization process; and the overlap method could not be assessed by the Rayleigh-Ritz method due to the difficulty in modeling the discrete thickness changes. Therefore the overlap design for the *RR/LDT* analysis used the prototype design found using the tow-drop design run, and was analyzed using the *LDT* tool with the overlap method.

**Table 3: Design Results for Rectangular Panel without Central Hole**

| Analysis      | Construction Method | Layup   | Buckling Load (lbs) | Relative increase |
|---------------|---------------------|---|---------------------|-------------------|
| <i>RR/LDT</i> | Straight            | $[\pm 45_2/\pm 30/\pm 45/\pm 15]_s$                   | 9479                | -                 |
| <i>STAGS</i>  | Straight            | $[\pm 60_3/0_4]_s$                                    | 9739                | 2.7%              |
| <i>RR/LDT</i> | Tow-drop            | $[\pm 45/0\pm <45 60>_2/0\pm <30 15>/0\pm <45 60>]_s$ | 10640               | -                 |
| <i>STAGS</i>  | Tow-drop            | $[\pm 45/0\pm <45 60>_2/0\pm <15 0>]_s$               | 10820               | 1.7%              |
| <i>RR/LDT</i> | Overlap             | $[\pm 45/0\pm <45 60>_2/0\pm <30 15>/0\pm <45 60>]_s$ | 14503               | -                 |
| <i>STAGS</i>  | Overlap             | $[90_2/0\pm <75 60>_4]_s$                             | 19175               | 32.2%             |

The results for the traditional straight fiber laminate reveal that though the buckling loads are relatively equal, the nature of the laminate is quite different. This is due to the difference in boundary conditions considered by the analysis during the optimization process. The present method, which uses the actual test conditions imposed on the finite element model, tends to produce designs with fibers running predominantly in the vertical direction to better withstand the bending deformation associated with clamped conditions at the top and bottom of the model. For the tow-drop method, the present results reaffirm the usefulness of the earlier design technique, since both analysis methods produce similar designs. For the tow-drop construction method, the main mechanism to improve the buckling load is to steer the loading toward the edges of the panel, which unloads the center section and delays the onset of instability. This feature is independent of the out-of-plane boundary conditions applied to the buckling mode, so that the best designs tend to possess similar tow-steered plies. The largest difference between the two analysis techniques occurs for the design of an overlap panel. Since the earlier overlap design was based on the tow-drop design, it was assumed that the load distribution would work in a similar manner to improve the buckling load. However, the new optimization runs that used the overlap construction method directly within *STAGS* indicate that even greater gains are attainable through the optimal placement of the overlap regions. The  $0\pm <75|60>$  overlap ply that dominates the design produces drastic thickness build-ups at the center of the panel, which is directly opposed to the established mechanism of directing the loads toward the edges of the panel. This is discussed in more detail once the results are presented for the panels with a hole.

The effect of the central hole is established in the data of Table 4 and Table 5.

**Table 4: Design Results for Rectangular Panel with Small (1.5" diameter) Central Hole**

| Analysis      | Construction Method | Layup   | Buckling Load (lbs) | Relative increase |
|---------------|---------------------|---|---------------------|-------------------|
| <i>RR/LDT</i> | Straight            | $[\pm 45_2/\pm 30/\pm 45/\pm 15]_s$                   | 8946                | -                 |
| <i>STAGS</i>  | Straight            | $[\pm 60_3/\pm 15/0_2]_s$                             | 9226                | 3.1%              |
| <i>RR/LDT</i> | Tow-drop            | $[\pm 45/0\pm <45 60>_2/0\pm <30 15>/0\pm <45 60>]_s$ | 10111               | -                 |
| <i>STAGS</i>  | Tow-drop            | $[\pm 45/0\pm <45 60>_3/0_2]_s$                       | 10258               | 1.5%              |
| <i>RR/LDT</i> | Overlap             | $[\pm 45/0\pm <45 60>_2/0\pm <30 15>/0\pm <45 60>]_s$ | 13211               | -                 |
| <i>STAGS</i>  | Overlap             | $[90_2/0\pm <75 60>_4]_s$                             | 17170               | 30.0%             |

**Table 5: Design Results for Rectangular Panel with Large (3" diameter) Central Hole**

| Analysis      | Construction Method | Layup   | Buckling Load (lbs) | Relative increase |
|---------------|---------------------|---|---------------------|-------------------|
| <i>RR/LDT</i> | Straight            | $[\pm 45_2/\pm 30/\pm 45/\pm 15]_s$                   | 8401                | -                 |
| <i>STAGS</i>  | Straight            | $[\pm 60_3/0_4]_s$                                    | 8894                | 5.9%              |
| <i>RR/LDT</i> | Tow-drop            | $[\pm 45/0\pm <45 60>_2/0\pm <30 15>/0\pm <45 60>]_s$ | 9508                | -                 |
| <i>STAGS</i>  | Tow-drop            | $[\pm 45/0\pm <45 60>_2/0\pm <30 45>/0\pm <15 0>]_s$  | 9769                | 2.7%              |
| <i>RR/LDT</i> | Overlap             | $[\pm 45/0\pm <45 60>_2/0\pm <30 15>/0\pm <45 60>]_s$ | 13119               | -                 |
| <i>STAGS</i>  | Overlap             | $[\pm 45/0\pm <60 75>_4]_s$                           | 17121               | 30.5%             |

As expected, increasing the hole size lowers the estimated buckling load for a given layup, such as the designs produced by the *RR/LDT* method. As before, the straight fiber designs using the *STAGS* analysis place the fibers more toward the vertical to withstand the higher bending loads due to the clamped ends, with small increases in the buckling loads. For the tow-drop panels, designs using the same families of tow-steered plies provide the best buckling loads, again with only small improvement over the earlier design technique.

The significant results occur for the design of the overlap panels. Note that for the panel with the large hole, the best design uses a  $0\pm <60|75>$  overlap ply to steer the loading toward the edges which are reinforced by the thickness build-up, which is the established mechanism discovered for variable stiffness panels. To illustrate this point graphically, a plot of the thickness distribution for the  $[\pm 45/0\pm <60|75>_4]_s$  layup is displayed in Figure 25 on the left. This plot was constructed by coloring each element according to the number of layers present at the element centroid, and ranges from 20 layers (light coloring) to 36 (darkest) where the intersection of the overlap regions occur.<sup>†††</sup> Note how the overlap regions approximate a series of interlocking stiffeners that surround the thinner interior section of the panel. The plot on the right in Figure 25 indicates the resulting distribution of the vertical stress resultant due to the applied loading. The darker regions indicate higher compressive stress, and the results indicate that the edges carry loads at least two times that of the thinner sections (above and below the hole). As discussed, this leads to higher buckling loads due to the reduced stress state within the interior of the panel.

Conversely, similar plots of the thickness distribution and vertical stress resultant are displayed in Figure 26 for the best *STAGS* stacking sequence design for the panel with a small hole, given in Table 4 as  $[90_2/0\pm <75|60>_4]_s$ . Now the integral stiffeners run down the center of the panel, building up the thickness around the central hole. Surprisingly, the higher stresses that are now directed to the center of the panel do not reduce the onset of stability. This is due to the fact that the large thickness increase effectively increases the bending stiffness at the center of the laminate so that buckling is less likely. In truth, it can be reasoned that since adding to the thickness of a laminate raises the in-plane stiffness proportionally ( $E_y \sim h$ ) while increasing the bending stiffness to the third power ( $D \sim h^3$ ), then the previous result should be expected. However this is not always the case for panel buckling, since the edge conditions and two-dimensional nature of the buckling mode complicate the interaction of the in-plane stress state and bending stiffness parameters. Therefore, it is surmised that the previous result depends highly on the size of the central hole, since the  $[90_2/0\pm <75|60>_4]_s$  layup does not exhibit the same increase for the panel with the larger hole size (15430 lbs). In other words, the large hole size is large enough to degrade the ability of the thicker center section to resist buckling, while for the panel with no hole and the smaller hole, the increased thickness improves the overall buckling response of the panel. Additionally, the

<sup>†††</sup> In actual practice during manufacture, the tow-steered plies would be staggered to smooth out the discrete nature of the thickness variation. This staggering technique leads to a better quality laminate without a significant change in the reported buckling loads.

$[\pm 45/0 \pm \langle 60/75 \rangle_4]_s$  layup, when analyzed with the small hole model, generates a buckling load of 16701 lbs, appreciably less than the design that lumps the thickness distribution in the center of the panel. Thus this result indicates that another mechanism may exist to improve the load-carrying capability for panels with central holes: namely, beefing up the area around the hole with substantial thickness increases. Toward this end, additional mechanical testing using tow-steered panels with such overlap regions is planned for the future, to see if this mechanism increases the panel performance. However, it should also be noticed that the greater thickness in the center of the panel increases the stresses around the cut-out (see the stress contours in Figure 26), which may indicate that material failure becomes a critical constraint.

### 5.3 Square Plate with Central Hole under In-plane Shear Load

The final design problem is for a square plate subjected to in-plane shear loading. This case is intended to investigate the potential of tow-steered designs under more complex loading, therefore optimization runs similar to those used for the rectangular panel under compression will be considered. Since the mechanisms for improvement of the buckling load under shear loading have not been investigated as thoroughly as normal loading, other design possibilities will also be investigated to fully explore the design space offered by tow-steered laminates.

The dimensions of the test section are 12 inches square, and optional hole sizes of the same diameter as for the rectangular panel under compression are allowed. Boundary conditions are constructed to correspond with actual testing conditions for a biaxial loading test fixture, as described in the investigation by Ambur et al.<sup>20</sup> The *STAGS* model used here is shown in Figure 27, where the shaded regions denote the loading frame used to apply the shear loading. The frame sections are connected with pins and are sturdy enough to remain straight during loading, so that the shear deformation shown to the right occurs from the opposing forces applied by the testing machine. For constant stiffness panels with no central hole, this produces a constant state of shear stress within the laminate.

For panels with holes and/or stiffness variation under shear loading, the load paths and stress distribution within the panel is not as intuitive as for simple in-plane compression. For example, the shear stress resultant for a constant stiffness panel with a large central hole is shown in Figure 28a. The darker shades represent higher shear stress (stresses within the frame sections have been removed for clarity), and indicate the complexity of the stress state around the circumference of the hole. The predominant buckling mode for the given loading is displayed in Figure 28b, where the contour lines represent the out-of-plane deformation of the panel. These results do not provide any straightforward indication of which stiffness variation will improve the buckling performance of the laminate. For a different perspective, the normal stress resultant rotated at an angle of  $-45$  degrees is calculated and shown as a contour plot in Figure 29. This stress resultant quantity better illustrates the variation of the compressive stresses that lead to buckling of the laminate, and will be used hereafter for the shear stress results. Using this diagonal normal stress resultant quantity as a guide, it is interesting to look at the changes in behavior when the prototype tow-steered panels manufactured from the earlier design studies are used for the laminate definition. Results for the buckling loads for these prototype designs for a plate with different hole sizes are given in Table 6 on the next page.

The variation of the diagonal normal stress resultant for the  $[\pm 45/0 \pm \langle 45/60 \rangle_2/0 \pm \langle 30/15 \rangle/0 \pm \langle 45/60 \rangle]_s$  layup using the tow-drop construction method is shown in Figure 30 for the panel with the large hole. Recall that this design possesses a horizontal stiffness variation and has fibers aligned more toward the vertical at the left and right edges of the panel. Though useful under axial compression, this stiffness configuration does not enhance the buckling performance under shear, in fact the buckling load decreases approximately 2% compared to the constant stiffness laminate. Furthermore, the distribution of the diagonal normal stresses seems largely unaffected by the stiffness variation when compared to the constant stiffness result. A corresponding plot of the diagonal normal stress resultant is shown for the

overlap panel design in Figure 31. Note how the integral stiffeners that arise due to the overlaps tend to carry more of the load than the thinner regions in between, though some areas near the center of the panel still exhibit the high levels of stress due to the stress concentration at the central hole. Thus the mechanism of steering the loading toward the edges does not seem as apparent here and may not apply for this loading case.

**Table 6: Analysis Results for Square Panel under Shear using Prototype Designs**

| Hole Size  | Construction Method | Layup   | Buckling Load (lbs) |
|------------|---------------------|---|---------------------|
| No hole    | Straight            | $[\pm 45_2/\pm 30/\pm 45/\pm 15]_s$                   | 26585               |
| Small hole |                     |   | 22858               |
| Large hole |                     |   | 18969               |
| No hole    | Tow-drop            | $[\pm 45/0\pm <45 60>_2/0\pm <30 15>/0\pm <45 60>]_s$ | 26088               |
| Small hole |                     |   | 22451               |
| Large hole |                     |   | 18603               |
| No hole    | Overlap             | $[\pm 45/0\pm <45 60>_2/0\pm <30 15>/0\pm <45 60>]_s$ | 31860               |
| Small hole |                     |   | 27227               |
| Large hole |                     |   | 22630               |

Design runs using *OLGA* along with the models displayed in Figure 27 were conducted for the square panel loaded under shear. The optimization parameters and laminate characteristics were identical to the ones used for the rectangular panel under axial compression. For the tow-steered design runs, the main studies used a horizontal stiffness variation (vertical variations being equivalent due to the symmetry of the geometry and loading). Additional designs were investigated that alternated the stiffness variation between the horizontal and vertical directions within one laminate to provide greater flexibility within the design space, though the resulting laminates did not perform as well as those with the horizontal variation and are not reported. Results for the horizontal stiffness variation are supplied in Table 7, where the relative increase is with respect to the prototype designs given in Table 6.

**Table 7: Design Results for Square Panel under Shear Loading using Horizontal Variation**

| Hole Size  | Construction Method | Layup                                    | Buckling Load (lbs) | Relative Increase |
|------------|---------------------|--|---------------------|-------------------|
| No hole    | Straight            | $[\pm 45_2/0_2/90_4]_s$                  | 26866               | 1.1%              |
| Small hole |                     | $[\pm 45_3/90_2/0_2]_s$                  | 23078               | 1.0%              |
| Large hole |                     | $[\pm 45_3/90_2/0_2]_s$                  | 19107               | 0.7%              |
| No hole    | Tow-drop            | $[\pm 45/0\pm <45 30>/0\pm <75 45>_3]_s$ | 27675               | 6.1%              |
| Small hole |                     | $[\pm 30/0\pm <75 45>_4]_s$              | 23771               | 5.9%              |
| Large hole |                     | $[\pm 45/0\pm <75 45>_4]_s$              | 19968               | 7.3%              |
| No hole    | Overlap             | $[\pm 45/0\pm <75 45>_4]_s$              | 105457              | 231%              |
| Small hole |                     | $[\pm 45/0\pm <75 45>_4]_s$              | 91155               | 235%              |
| Large hole |                     | $[\pm 45/0\pm <75 45>_4]_s$              | 73326               | 224%              |

Note that the hole size does not greatly affect the stacking sequence design, though the magnitudes of the buckling loads differ appreciably. For the constant stiffness designs, only a slight increase with respect to the prototype design is found. The tow-drop method generates moderate improvement with respect to its

corresponding prototype design, though the buckling loads are only slightly above those of the best straight fiber laminate. Overlap designs utilize the same dominant tow-steered ply ( $0\pm<75|45>$ ) as those that use the tow-drop method, which produces a thickness build-up in the center of the panel. However, the resulting buckling loads for the overlap method exhibit a substantial increase over the other designs.

To investigate the mechanism behind this improvement, the large hole model using the overlap construction technique is analyzed to determine the prebuckling state and buckling mode of the structure. The thickness distribution is shown in Figure 32, along with the resulting shear stress resultant for the prebuckling state. Note the extreme thickness build-up due to the  $0\pm<75|45>$  ply, where the middle section is often twice the thickness of the edge regions. However, the shear stress variation displayed in Figure 32 indicates that this does not automatically translate into the thicker areas carrying the majority of the loading. Instead, the shear loading paths seem to follow the curves of the thickness build-up from the edges that are loaded in shear and then smooth out at the thicker center of the panel. This is even more apparent when the diagonal normal stress variation is displayed, as in Figure 33, which indicates how the stiffer regions carry the higher normal stresses. Thus the thicker center is better able to withstand the onset of instability at the center of the panel (since it is a thicker laminate there) without a corresponding increase in the load level. This clearly exemplifies the possibilities that tow-steering can achieve: altering the stress state to reduce the level of stress in critical areas while simultaneously improving the resistance of the laminate to failure.

Validation of the tow-steering designs for shear loading is underway, with mechanical tests planned for the prototype laminates given in Table 6. These designs were chosen because they had already been manufactured through earlier projects. Correlation of the testing results with the finite element predictions provided here will reaffirm the ability of the tow-steering concepts to improve the performance of composite panels under a variety of loading conditions.

## 6.0 Concluding Remarks

The ability to use finite element models within an automated design environment based on Genetic Algorithm optimization techniques is a valuable accomplishment for laminate design. Inclusion of elastic tailoring through the tow-steering definitions makes the laminate analysis tool even more useful, capable of fully exploring the potential of the superior unidirectional properties of fiber-reinforced composite materials for a variety of geometries and loading conditions. Indeed, the results produced by this investigation have revealed several new mechanisms that are capable of improving buckling loads for composite panels under in-plane loading. The generality of the tool and the availability of user-written subroutines to define the elastic tailoring configurations within *STAGS* enables new applications of the variable stiffness design concepts to be quickly implemented within the design environment. Thus this design tool provides an excellent groundwork into more detailed design of tow-steered laminates.

## Figures



Figure 1: Photograph of Viper Tow Placement System (courtesy of Cincinnati Machine)

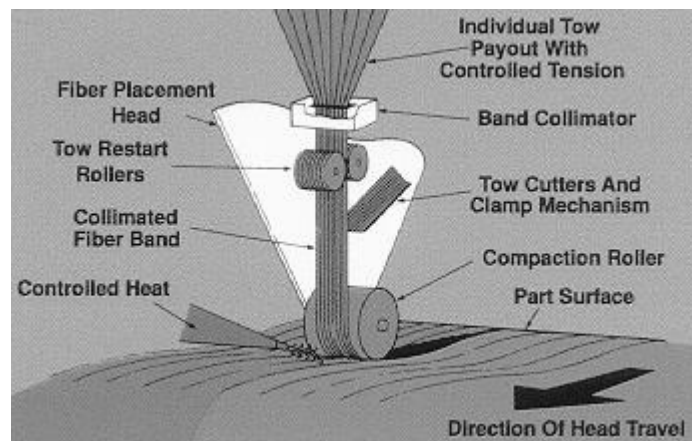


Figure 2: Schematic of Viper Tow Placement System (courtesy of Cincinnati Machine)

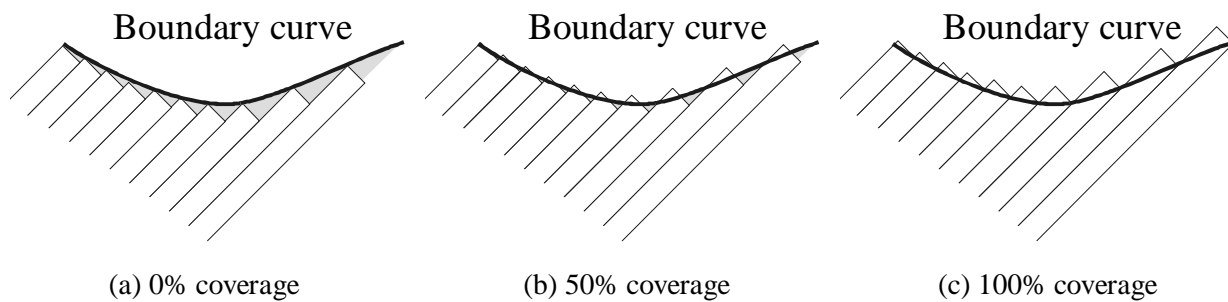
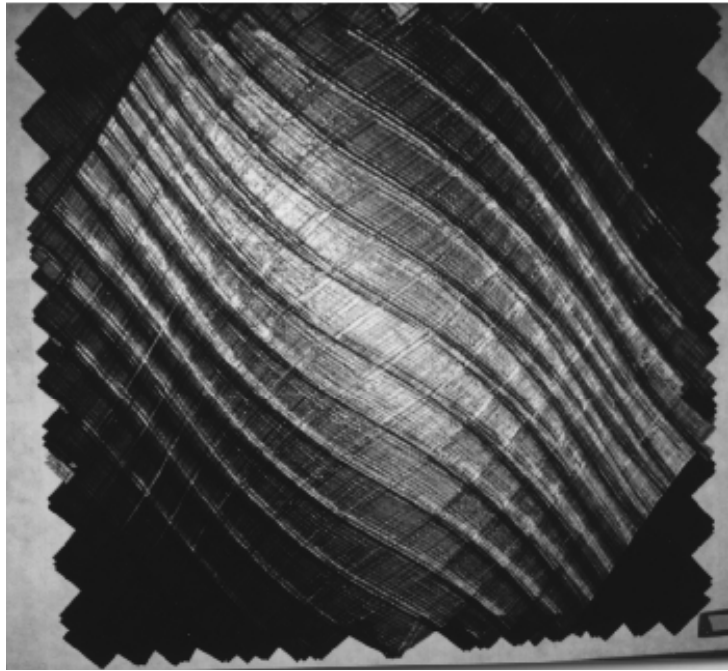
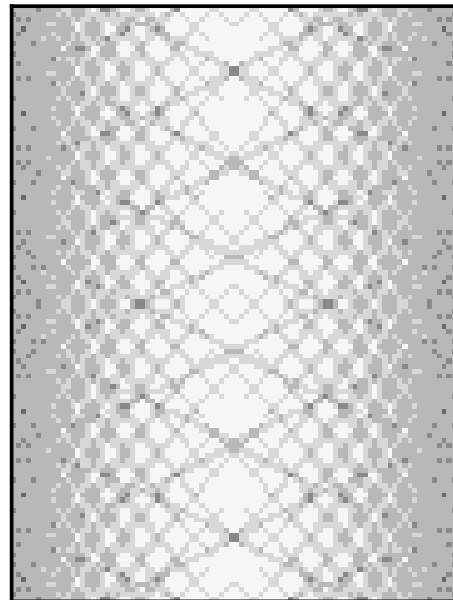
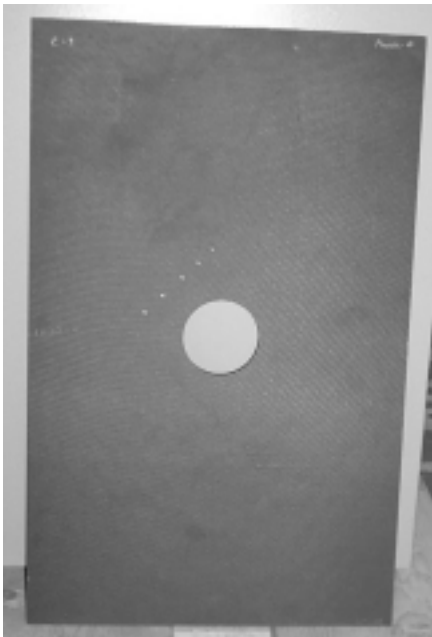


Figure 3: Tow drop locations using different coverage values





**Figure 4: Fabricated panel using integral stiffeners**



**Figure 5: Fabricated panel and thickness estimate for laminate with staggered thickness build-ups**

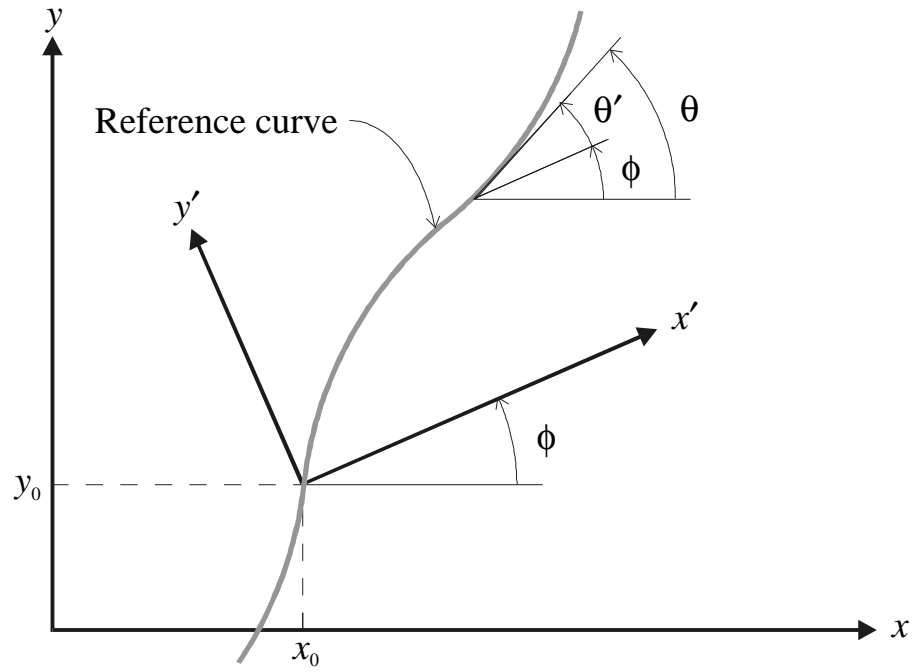


**Figure 6: Rotated axes for stiffness variation definition**

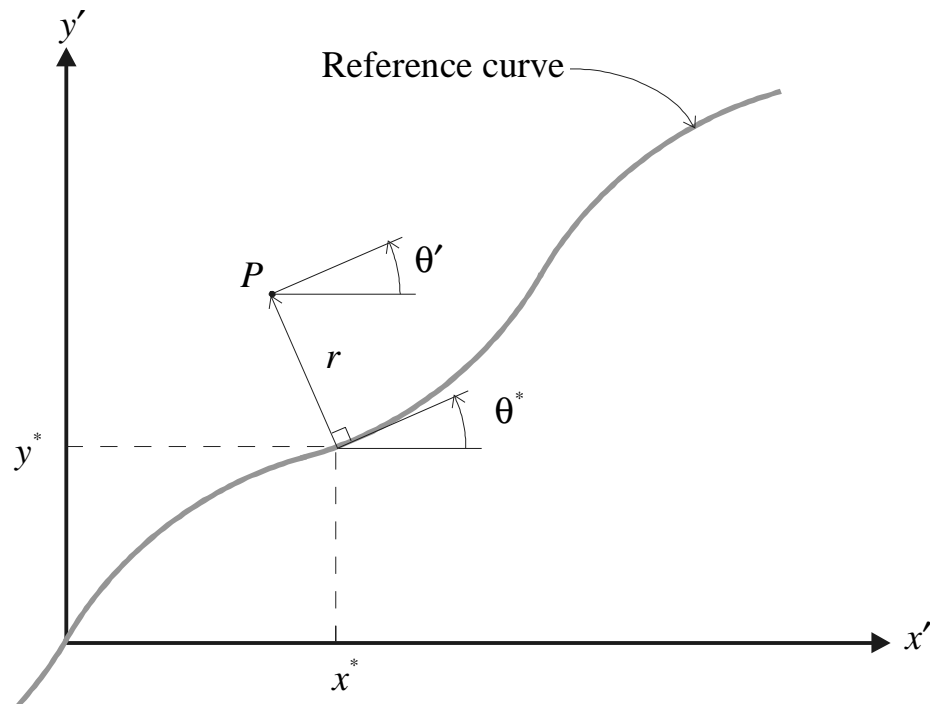


**Figure 7: Reference path in directional coordinates**

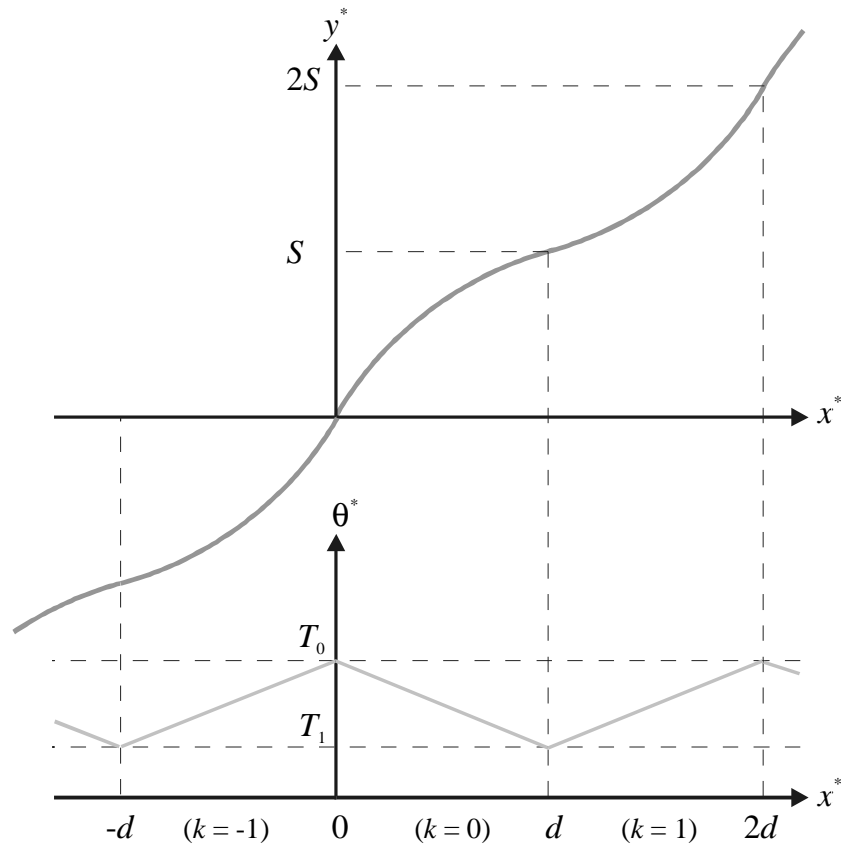


**Figure 8: Reference curve function based on linear angle variation**

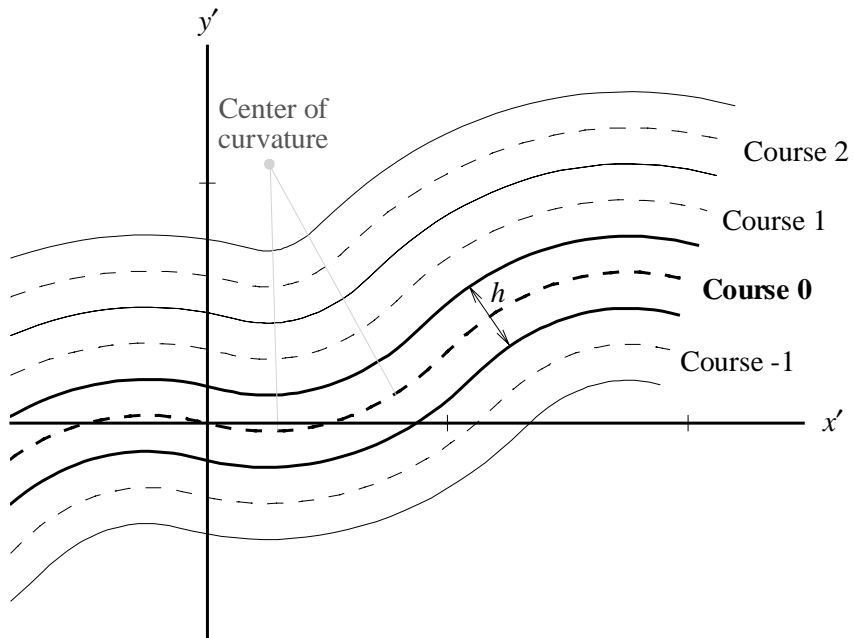


**Figure 9: Configuration for 0<-15|45> parallel method ply**

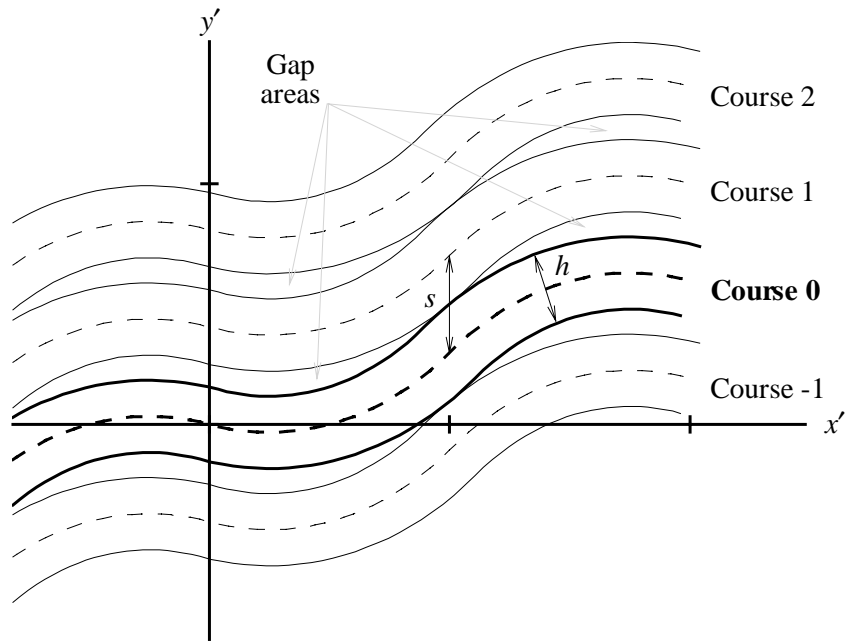


Figure 10: Shifted configuration for 0<-15|45> ply with zero overlap

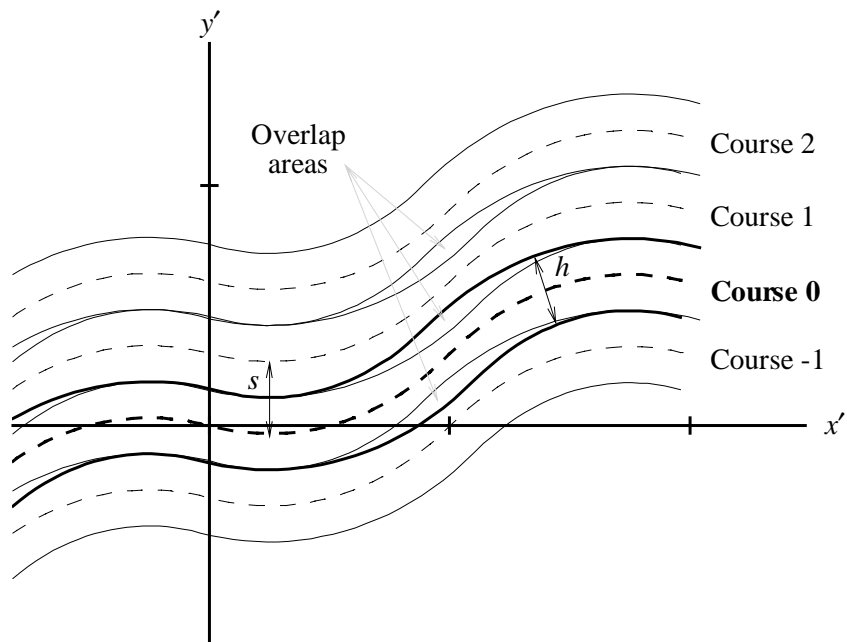
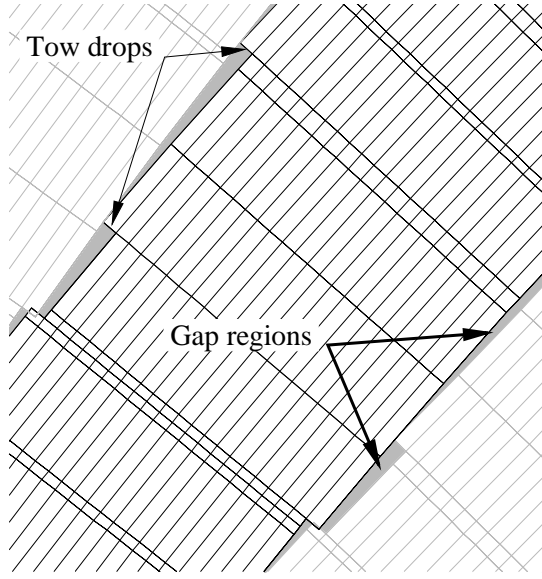
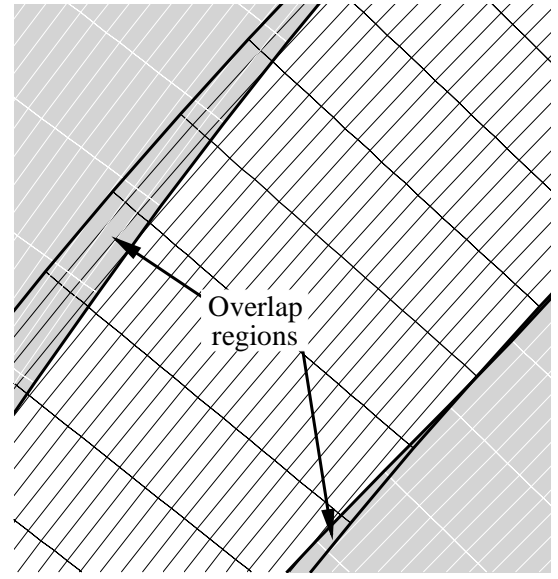


Figure 11: Shifted configuration for 0<-15|45> ply with zero gap



Tow-drop method



Overlap method

Figure 12: Close-ups of overlap region using both shifted methods

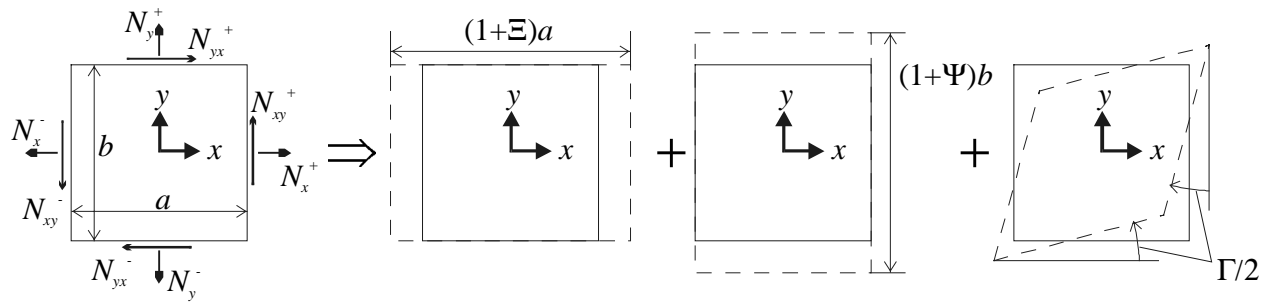
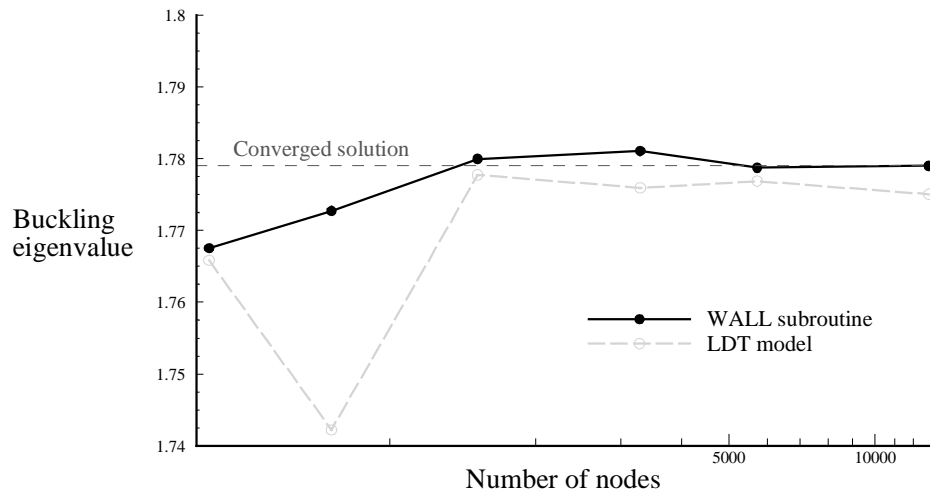
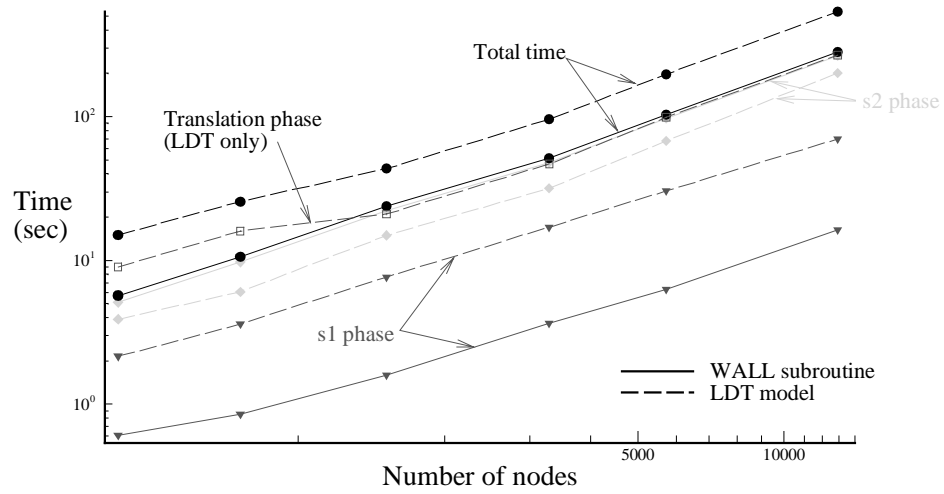


Figure 13: Loading and deformation for straight edge rectangular panel



**Figure 14: Convergence of eigenvalue for WALL and *LDT* techniques**



**Figure 15: Execution times for WALL and *LDT* techniques**

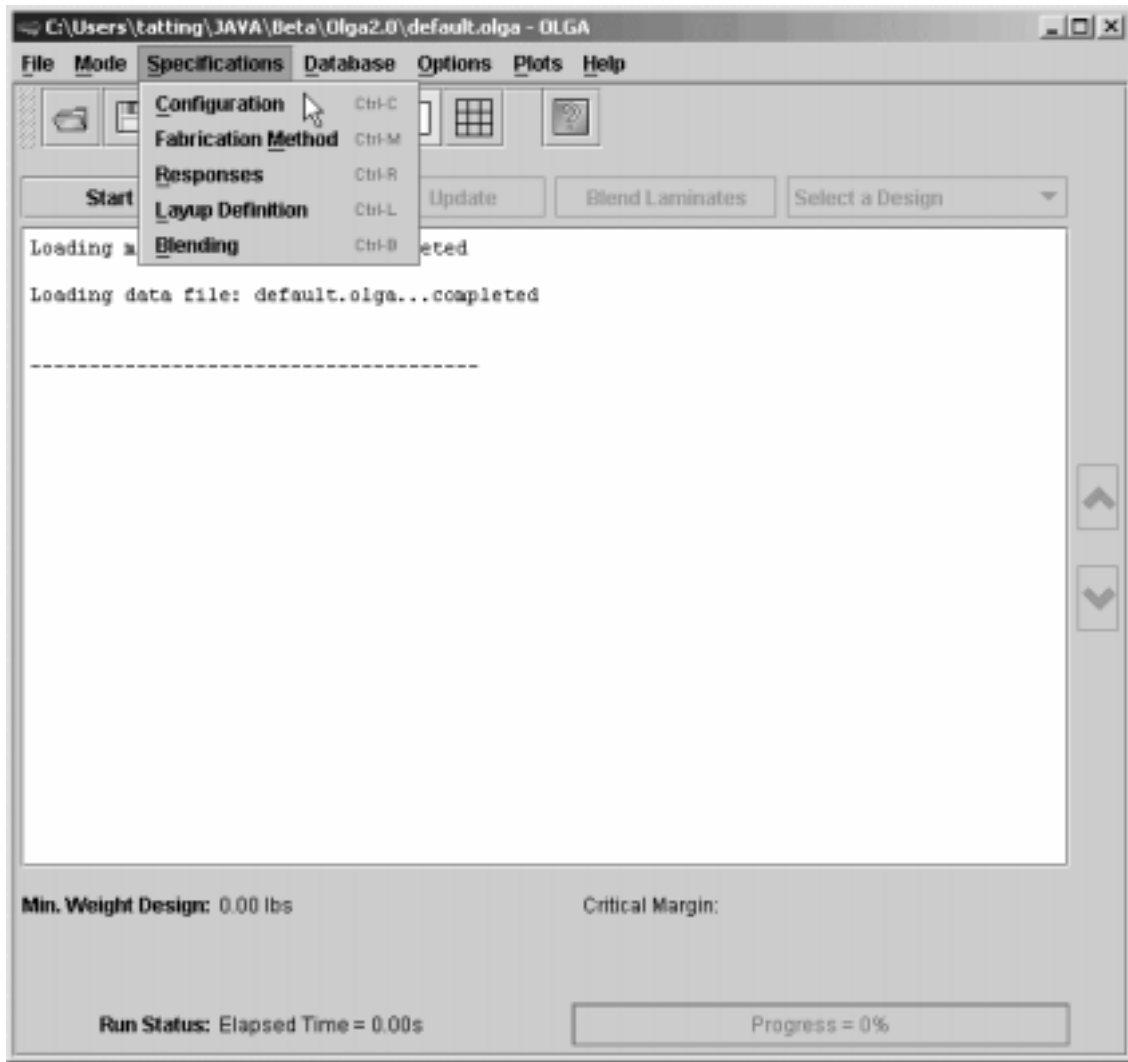


Figure 16: OLGA main dialog

**Panel Configuration - OLGA**

**Panel Layout:**

Number of Panels: X-dir:  Y-dir:

☒ Hide de-activated panels

☒ Panel activated

☐ Monolithic ☒ Sandwich

**Geometry:**

Length (x-dir):  Xc:

Height (y-dir):  Yc:

Press the "Layout Panels" button to update the configuration

**Sandwich core:**

☒ Design thickness

Min. thickness:

Max. thickness:

**Loading:**

Nx:  Ny:  Nyz:

Use negative values for compressive loads

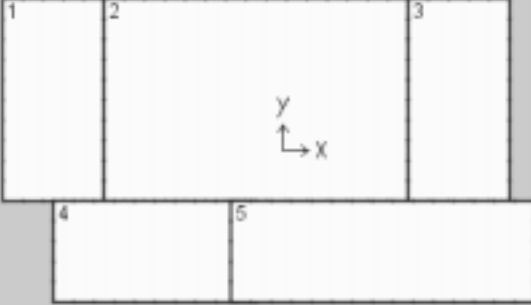


Figure 17: OLGA panel configuration dialog



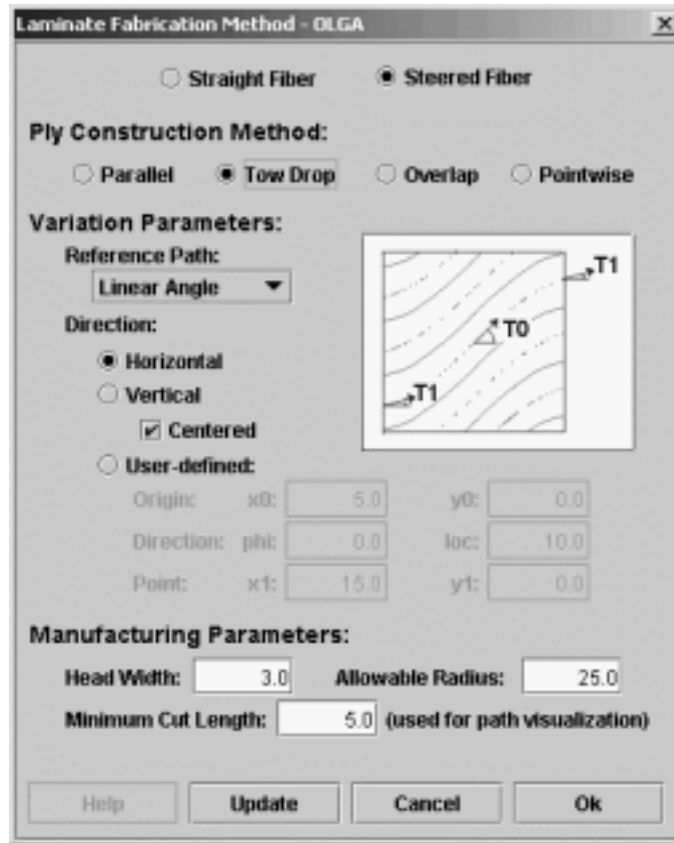


Figure 18: OLGA fabrication dialog

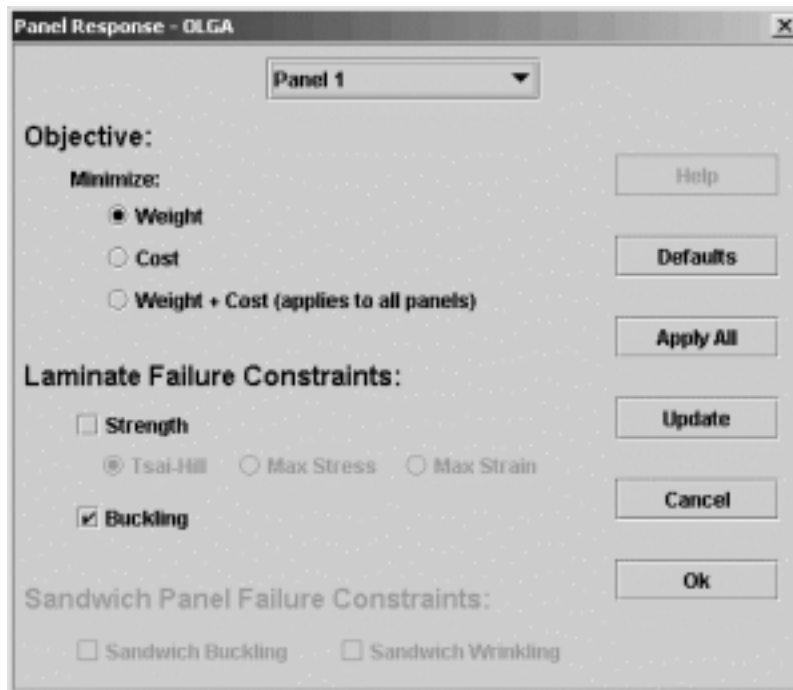


Figure 19: OLGA responses dialog

Layup Definition - OLGA

Panel 1

Laminate Stacking Sequence: Symmetric ☒

Num. Plies ☐ Min. Plies ☐ Max. Thickness ☐ Min. Thickness ☐ Contiguous Plies

20

☐ Unbalanced ☐ Balanced ☒ Two-ply stacks Outer plies constant angle

Ply Orientations:

| Select                              | Orientation | Max. % | Min. % |
|-------------------------------------|-------------|--------|--------|
| <input checked="" type="checkbox"/> | 0°          | 100.0  | 0.0    |
| <input checked="" type="checkbox"/> | ±15°        | 100.0  | 0.0    |
| <input checked="" type="checkbox"/> | ±30°        | 100.0  | 0.0    |
| <input checked="" type="checkbox"/> | ±45°        | 100.0  | 0.0    |
| <input checked="" type="checkbox"/> | ±60°        | 100.0  | 0.0    |
| <input checked="" type="checkbox"/> | ±75°        | 100.0  | 0.0    |
| <input checked="" type="checkbox"/> | 90°         | 100.0  | 0.0    |

☒ Use positive and negative angles

Materials: ☒ Composite ☐ Core

| Select                              | Material Name  |
|-------------------------------------|----------------|
| <input checked="" type="checkbox"/> | Graphite-Epoxy |
| <input type="checkbox"/>            | Kevlar-Epoxy   |
| <input type="checkbox"/>            | Glass-Epoxy    |

Select All Unselect All Database

Help Defaults Apply All Update Cancel Ok

Figure 20: OLGA layup definition dialog

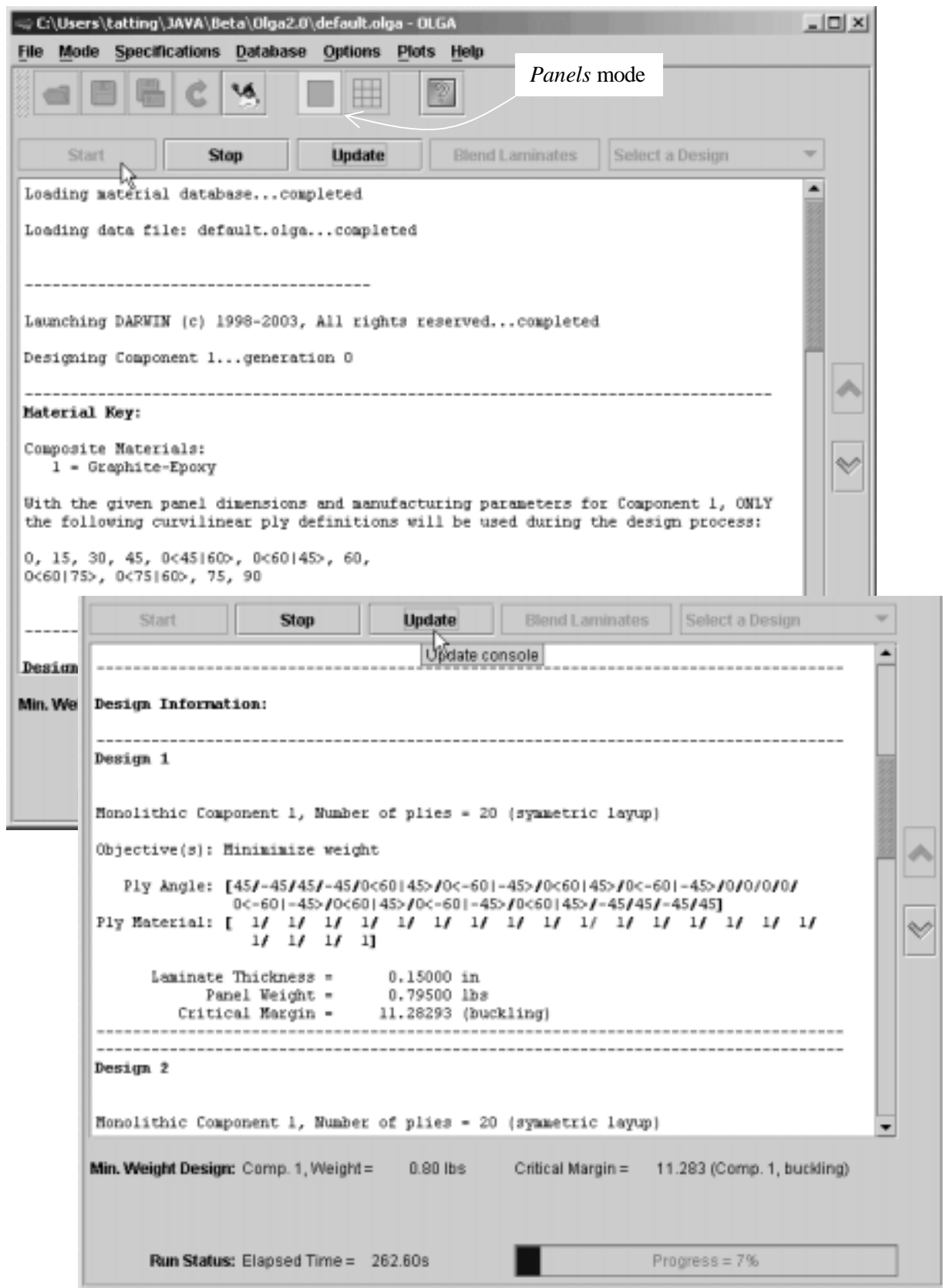
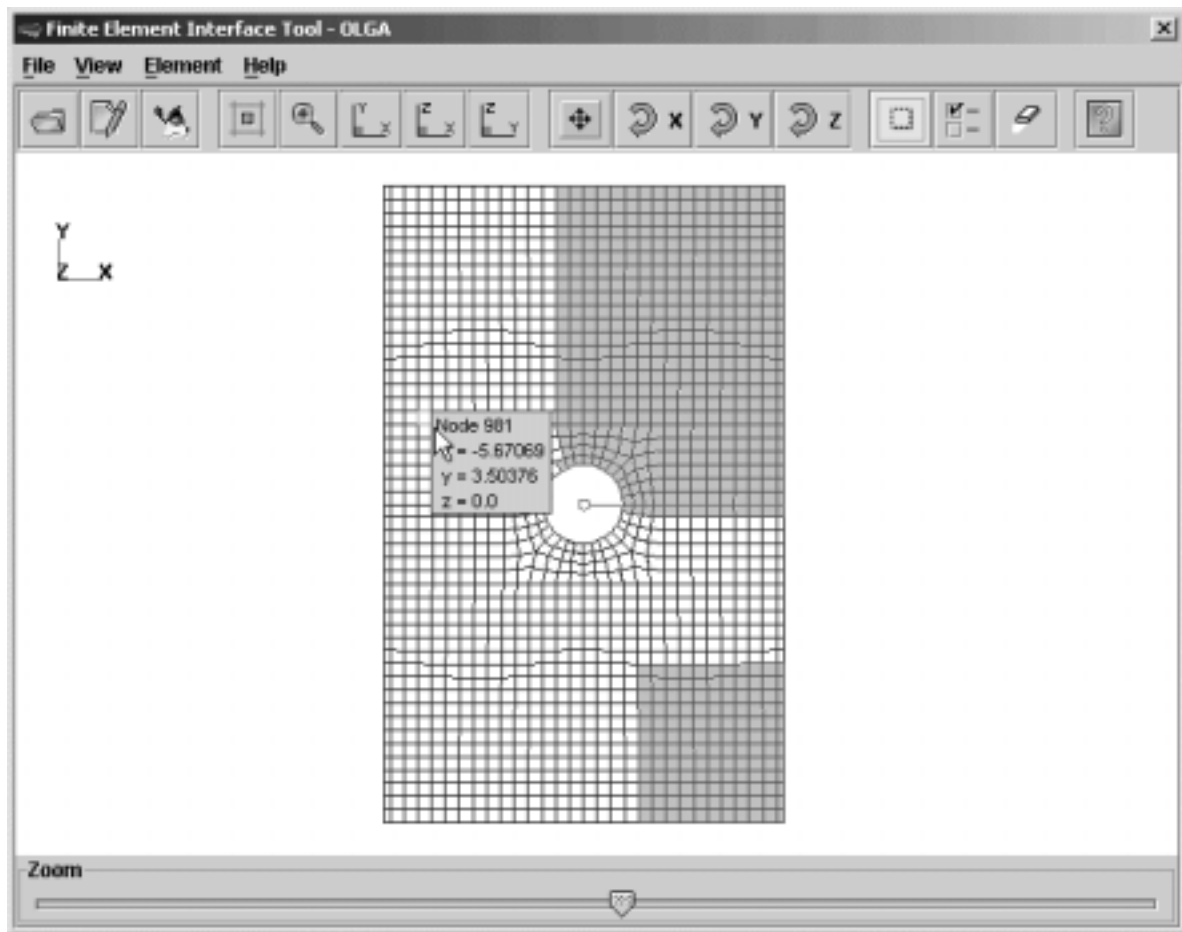
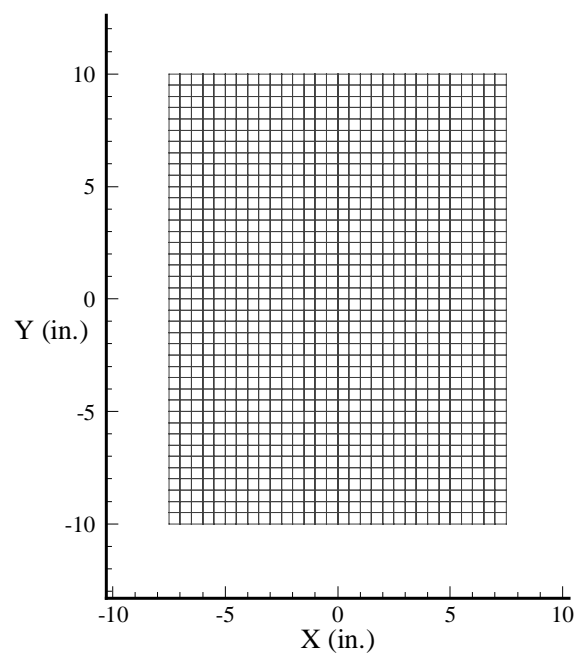


Figure 21: OLGA main dialog during execution



**Figure 22: OLGA finite element model interface dialog**



**Figure 23: Finite element mesh for simply-supported panel**

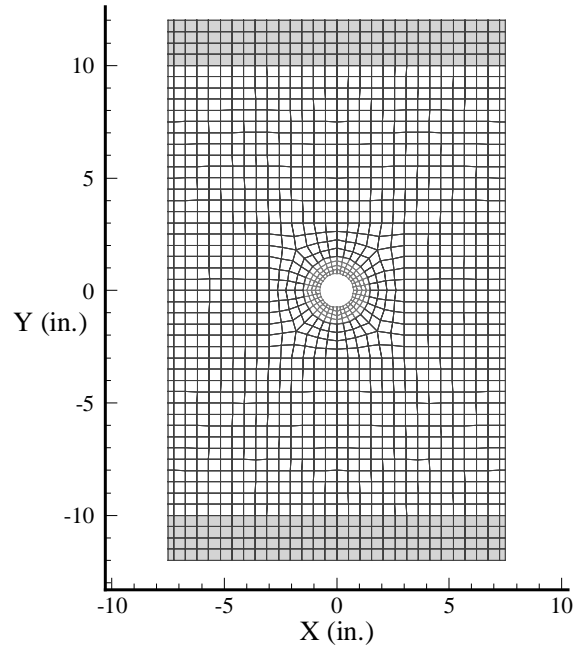


**Figure 24: Finite element mesh for panel with central hole**

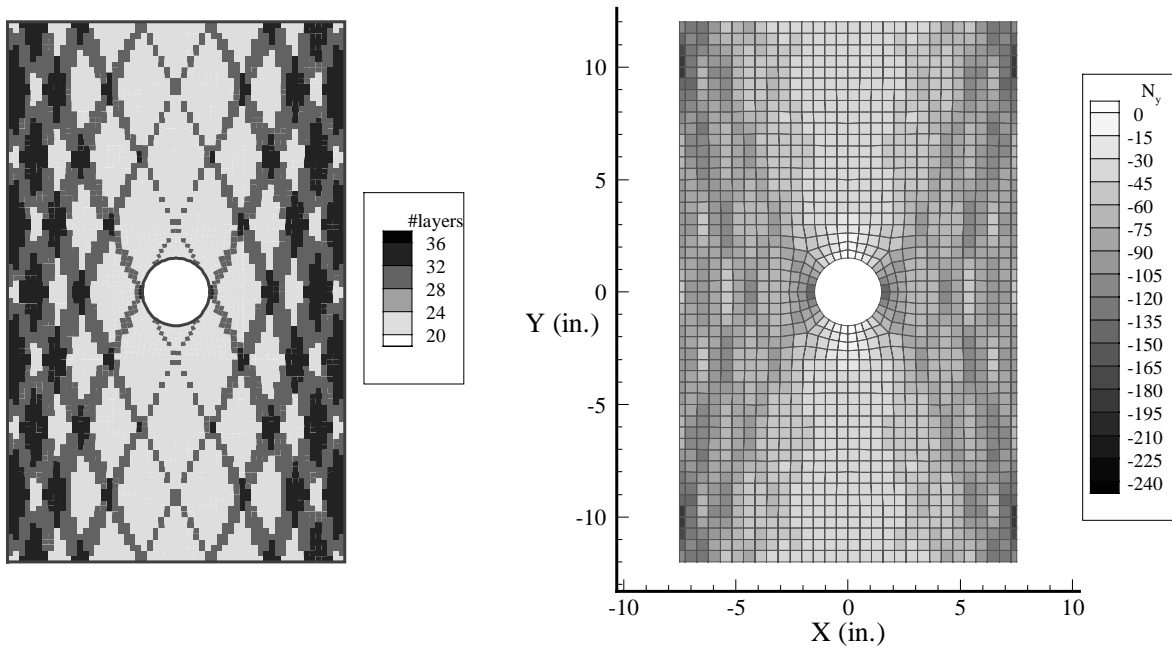


**Figure 25: Thickness distribution and prebuckling stress resultant  $N_y$  for panel with large hole**

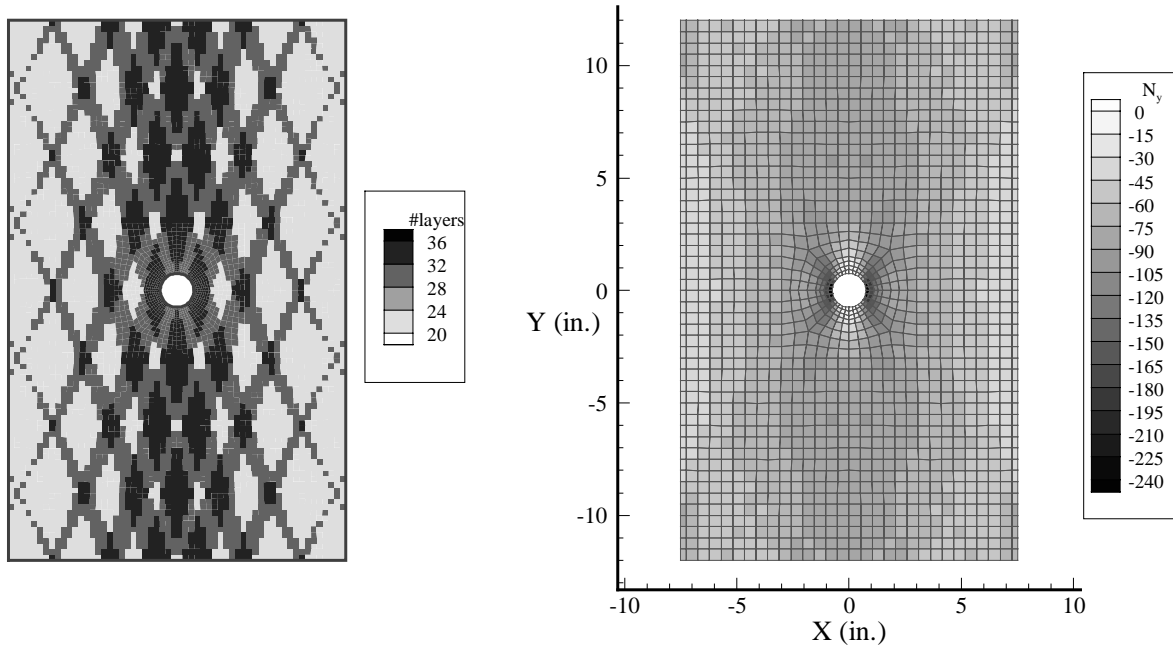


**Figure 26: Thickness distribution and prebuckling stress resultant  $N_y$  for panel with small hole**

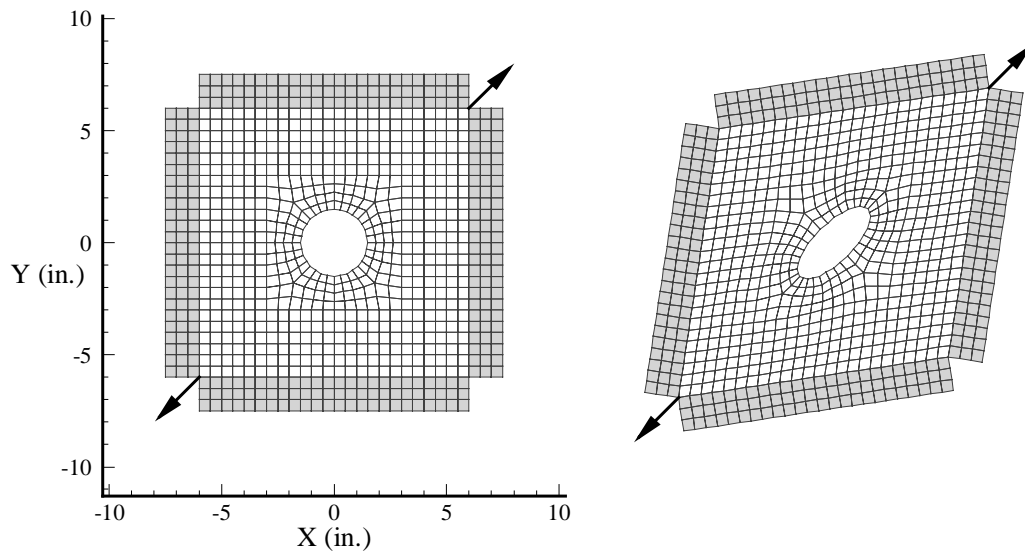
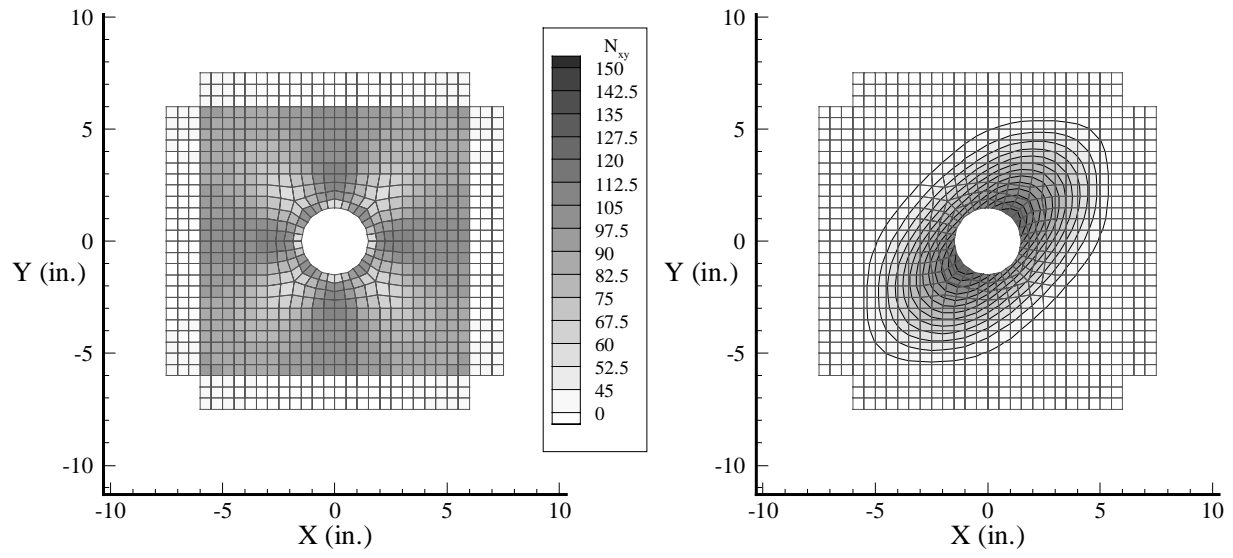


**Figure 27: Finite element mesh and intended deformation for square panel under shear**



(a) Shear Stress Resultant (b) Dominant Buckling Mode  
**Figure 28: Shear stress distribution and buckling mode for constant stiffness square panel**

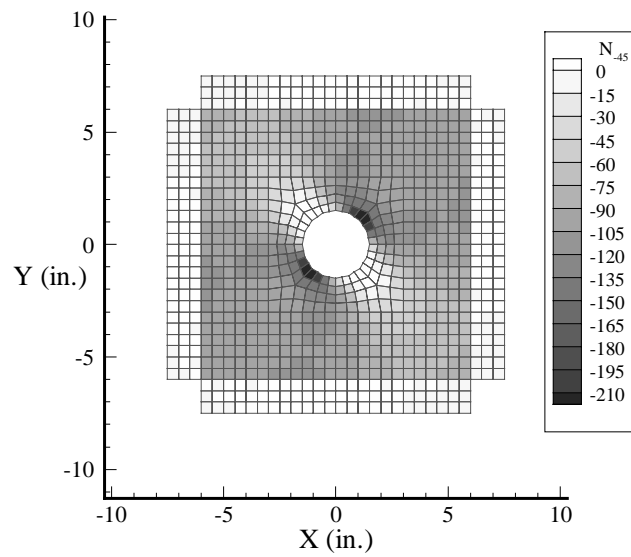


**Figure 29: Diagonal normal stress distribution for square panel with prototype constant stiffness design**

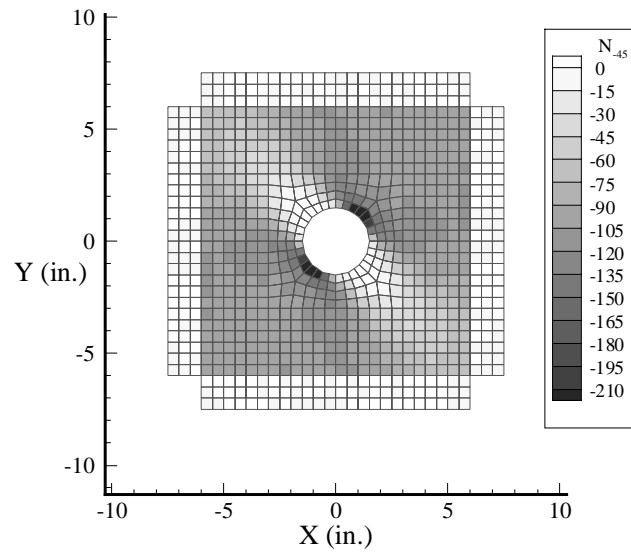


**Figure 30: Diagonal normal stress distribution for square panel with prototype tow-drop design**

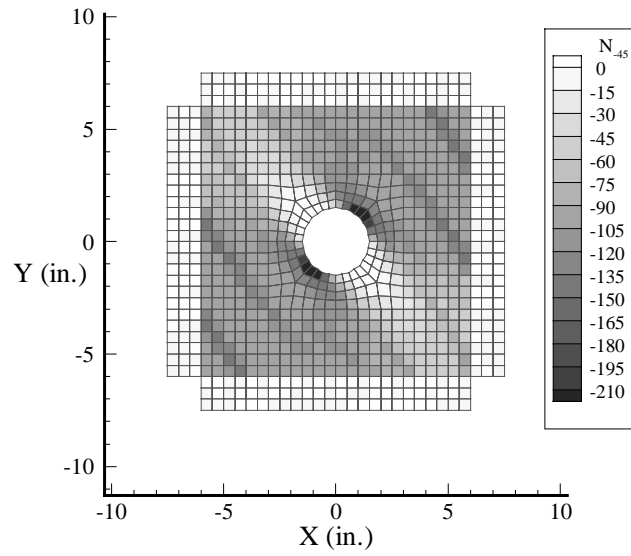


**Figure 31: Diagonal normal stress distribution for square panel with prototype overlap design**



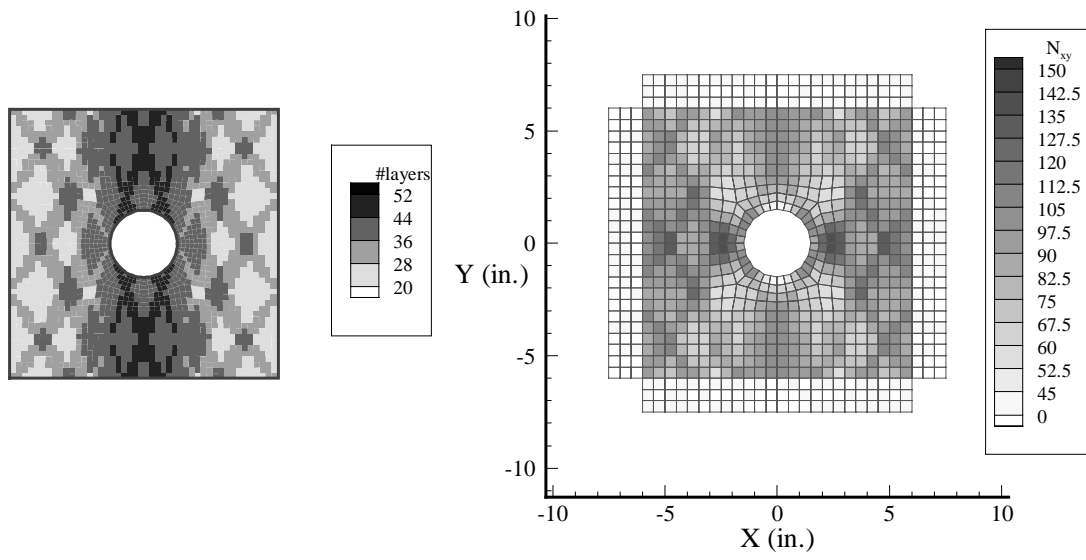


**Figure 32: Thickness distribution and shear stress resultant for square panel with large hole using optimal overlap design**

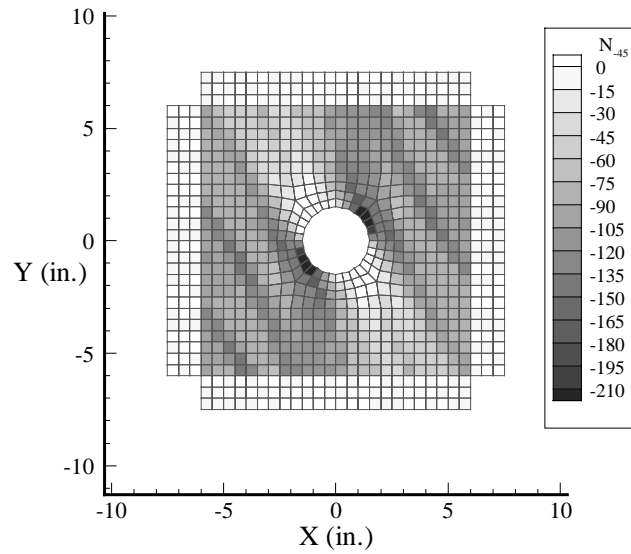


**Figure 33: Diagonal normal stress resultant for square panel with large hole using optimal overlap design**

## References

1. Yau, S. S., and Chou, T. W., "Strength of Woven-Fabric Composites with Drilled and Molded Holes," Composite Materials Testing and Design, ASTM STP-972, American Society for Testing and Materials, Philadelphia, PA, 1988, pp. 423-437.
2. Hyer, M. W., and Charette, R. F., "The Use of Curvilinear Fiber Format in Composite Structure Design," Proceedings of the 30<sup>th</sup> AIAA/ASME/ASCE/AHS/ASC Structures, Structural Dynamics and Materials (SDM) Conference, New York, NY, 1989, paper no. 1404.
3. Hyer, M. W., and Lee, H. H., "The Use of Curvilinear Fiber Format to Improve Buckling Resistance of Composite Plates with Central Holes," Composite Structures, Vol. 18, 1991, pp. 239-261.
4. Nagendra, S., Kodiyalam, A., Davis, J. E., and Parthasarathy, V. N., "Optimization of Tow Fiber Paths for Composite Design," Proceedings of the 36<sup>th</sup> AIAA/ASME/ASCE/AHS/ASC Structures, Structural Dynamics and Materials (SDM) Conference, New Orleans, LA, April 1995, paper no. 1275.
5. Waldhart, C. J., Gürdal, Z., and Ribbens, C., "Analysis of Tow Placed, Parallel Fiber, Variable Stiffness Laminates," Proceedings of the 37<sup>th</sup> AIAA/ASME/ASCE/AHS/ASC Structures, Structural Dynamics and Materials (SDM) Conference, Salt Lake City, UT, April 1996, paper no. 1569.
6. Tatting, B. F., and Gürdal, Z., Design and Manufacturing of Elastically Tailored Tow Placed Plates, NASA/CR 2002-211919, August 2002.
7. Evans, D. O., Vaniglia, M. M., and Hopkins, P. C., "Fiber Placement Process Study," 34<sup>th</sup> International SAMPE Symposium, May 1989.
8. Tatting, B. F., and Gürdal, Z., "Design and Manufacture of Tow-Placed Variable Stiffness Composite Laminates with Manufacturing Considerations," Proceedings of the 13<sup>th</sup> U.S. National Congress of Applied Mechanics (USNCAM), Gainesville, FL, 1998.
9. Wu, K. C., and Gürdal, Z., "Thermal Testing of Tow-Placed Variable Stiffness Panels," Proceedings of the 42<sup>nd</sup> AIAA/ASME/ASCE/AHS/ASC Structures, Structural Dynamics and Materials (SDM) Conference, Seattle, WA, April 2001, paper no. 1190.
10. Wu, K. C., Gürdal, Z., and Starnes, J. H., "Buckling and Postbuckling of Tow-Placed Variable Stiffness Panels," Proceedings of the 43<sup>rd</sup> AIAA/ASME/ASCE/AHS/ASC Structures, Structural Dynamics and Materials (SDM) Conference, Denver, CO, April 2002, paper no. 1512.
11. Gürdal, Z., and Olmedo, R., "In-Plane Response of Laminates with Spatially Varying Fiber Orientations: Variable Stiffness Concept," AIAA Journal, Vol. 31, (4), April 1993, pp. 751-758.
12. Olmedo, R., and Gürdal, Z., "Buckling Response of Laminates with Spatially Varying Fiber Orientations," Proceedings of the 34<sup>th</sup> AIAA/ASME/ASCE/AHS/ASC Structures, Structural Dynamics and Materials (SDM) Conference, La Jolla, CA, April 1993, paper no. 1567.
13. Jones, R. M., Mechanics of Composite Materials, Hemisphere Publishing Corporation, New York, NY, 1975, pp. 147-187.
14. Tatting, B. F., Gürdal, Z., "Analysis and Design of Tow-Steered Variable Stiffness Composite Laminates," Proceedings of the American Helicopter Society Hampton Roads Chapter, Structure Specialists' Meeting, Williamsburg, VA, October 2001.
15. Rankin, C. C., Brogan, F. A., Loden, W. A., and Cabiness, H. D., "STAGS Users Manual," Lockheed Martin Missiles & Space Co., Inc., Report LMSC P032594, June 2000.
16. Ellis, T. M. R., Philips, I. R., and Lahey, T. M., Fortran 90 Programming, Addison-Wesley Publishing Company Inc., Reading, MA, 1998, pp. 545-556.
17. Soremekun, G. A. E., and Gürdal, Z., "Advanced Genetic Algorithms for Designing Complex Laminated Structures," Proceedings of the American Helicopter Society Hampton Roads Chapter, Structure Specialists' Meeting, Williamsburg, VA, October 2001.

18. Eckel, B., Thinking in Java, Prentice Hall PTR, Upper Saddle River, NJ, 1998.
19. Gürdal, Z., Haftka, R.T., and Hajela, P., Design and Optimization of Laminated Composite Materials, John Wiley and Sons, Inc., New York, NY, 1999, pp. 185-218.
20. Ambur, D. R., Jaunky, N., Davila, C. G., and Hilburger, M., "Progressive Failure Studies of Composite Panels with and Without Cutouts," Proceedings of the 42<sup>nd</sup> AIAA/ASME/ASCE/AHS/ASC Structures, Structural Dynamics and Materials (SDM) Conference, Seattle, WA, April 2001, paper no. 1182.

| REPORT DOCUMENTATION PAGE   |             |                   |                               |  | Form Approved<br>OMB No. 0704-0188   |  |
|---|-------------|-------------------|-------------------------------|--|--|--|
| <p>The public reporting burden for this collection of information is estimated to average 1 hour per response, including the time for reviewing instructions, searching existing data sources, gathering and maintaining the data needed, and completing and reviewing the collection of information. Send comments regarding this burden estimate or any other aspect of this collection of information, including suggestions for reducing this burden, to Department of Defense, Washington Headquarters Services, Directorate for Information Operations and Reports (0704-0188), 1215 Jefferson Davis Highway, Suite 1204, Arlington, VA 22202-4302. Respondents should be aware that notwithstanding any other provision of law, no person shall be subject to any penalty for failing to comply with a collection of information if it does not display a currently valid OMB control number.</p> <p><b>PLEASE DO NOT RETURN YOUR FORM TO THE ABOVE ADDRESS.</b></p>   |             |                   |                               |  |  |  |
| 1. REPORT DATE (DD-MM-YYYY)   |             | 2. REPORT TYPE    |                               | 3. DATES COVERED (From - To)                                     |  |  |
| 01- 12 - 2003   |             | Contractor Report |                               |  |  |  |
| 4. TITLE AND SUBTITLE<br>Automated Finiet Element Analysis of Elastically-Tailored Plates   |             |                   |                               | 5a. CONTRACT NUMBER  |  |  |
|   |             |                   |                               | NAS1-00135   |  |  |
|   |             |                   |                               | 5b. GRANT NUMBER   |  |  |
|   |             |                   |                               | 5c. PROGRAM ELEMENT NUMBER                                       |  |  |
| 6. AUTHOR(S)<br>Tatting, Brian F.; and Gürdal, Zafer  |             |                   |                               | 5d. PROJECT NUMBER   |  |  |
|   |             |                   |                               | 5e. TASK NUMBER  |  |  |
|   |             |                   |                               | 5f. WORK UNIT NUMBER   |  |  |
|   |             |                   |                               | 23-719-55-TA   |  |  |
| 7. PERFORMING ORGANIZATION NAME(S) AND ADDRESS(ES)<br>NASA Langley Research Center<br>Hampton, VA 23681-2199  |             |                   |                               | 8. PERFORMING ORGANIZATION<br>REPORT NUMBER                      |  |  |
| 9. SPONSORING/MONITORING AGENCY NAME(S) AND ADDRESS(ES)<br>National Aeronautics and Space Administration<br>Washington, DC 20546-0001   |             |                   |                               | 10. SPONSOR/MONITOR'S ACRONYM(S)<br><br>NASA                     |  |  |
|   |             |                   |                               | 11. SPONSOR/MONITOR'S REPORT<br>NUMBER(S)<br>NASA/CR-2003-212679 |  |  |
| 12. DISTRIBUTION/AVAILABILITY STATEMENT<br>Unclassified - Unlimited<br>Subject Category 39<br>Availability: NASA CASI (301) 621-0390      Distribution: Nonstandard   |             |                   |                               |  |  |  |
| 13. SUPPLEMENTARY NOTES<br>Tatting: ADOPTTECH, Inc.; Gürdal: Virginia Polytechnic Institute and State University<br>Technical Monitor: Dawn C. Jegley<br>An electronic version can be found at <a href="http://techreports.larc.nasa.gov/ltrs/">http://techreports.larc.nasa.gov/ltrs/</a> or <a href="http://ntrs.nasa.gov">http://ntrs.nasa.gov</a>   |             |                   |                               |  |  |  |
| 14. ABSTRACT<br>A procedure for analyzing and designing elastically tailored composite laminates using the STAGS finite element solver has been presented. The methodology used to produce the elastic tailoring, namely computer-controlled steering of unidirectionally reinforced composite material tows, has been reduced to a handful of design parameters along with a selection of construction methods. The generality of the tow-steered ply definition provides the user a wide variety of options for laminate design, which can be automatically incorporated with any finite element model that is composed of STAGS shell elements. Furthermore, the variable stiffness parameterization is formulated so that manufacturability can be assessed during the design process, plus new ideas using tow steering concepts can be easily integrated within the general framework of the elastic tailoring definitions. Details for the necessary implementation of the tow-steering definitions within the STAGS hierarchy is provided, and the format of the ply definitions is discussed in detail to provide easy access to the elastic tailoring choices. Integration of the automated STAGS solver with laminate design software has been demonstrated, so that the large design space generated by the tow-steering options can be traversed effectively. Several design problems are presented which confirm the usefulness of the design tool as well as further establish the potential of tow-steered plies for laminate design. |             |                   |                               |  |  |  |
| 15. SUBJECT TERMS<br>Curvilinear fibers; Compression; Shear; Composite; Graphite-epoxy; Optimization; Tow-steering  |             |                   |                               |  |  |  |
| 16. SECURITY CLASSIFICATION OF:   |             |                   | 17. LIMITATION OF<br>ABSTRACT | 18. NUMBER<br>OF<br>PAGES  | 19a. NAME OF RESPONSIBLE PERSON  |  |
| a. REPORT   | b. ABSTRACT | c. THIS PAGE      |                               |  | STI Help Desk (email: <a href="mailto:help@sti.nasa.gov">help@sti.nasa.gov</a> ) |  |
| U   | U           | U                 | UU                            | 52   | 19b. TELEPHONE NUMBER (Include area code)<br>(301) 621-0390                      |  |